

# Optimized Laser Models with Heisenberg-Limited Coherence and Sub-Poissonian Beam Photon Statistics

L. A. Ostrowski,<sup>\*</sup> T. J. Baker, S. N. Saadatmand, and H. M. Wiseman<sup>†</sup>

*Centre for Quantum Dynamics, Griffith University,  
Yuggera Country, Brisbane, Queensland 4111, Australia*

(Dated: September 1, 2022)

Recently it has been shown that it is possible for a laser to produce a stationary beam with a coherence (quantified as the mean photon number at spectral peak) which scales as the fourth power of the mean number of excitations stored within the laser, this being quadratically larger than the standard or Schawlow-Townes limit [1]. Moreover, this was analytically proven to be the ultimate quantum limit (Heisenberg limit) scaling under defining conditions for CW lasers, plus a strong assumption about the properties of the output beam. In Ref. [2], we show that the latter can be replaced by a weaker assumption, which allows for highly sub-Poissonian output beams, without changing the upper bound scaling or its achievability. In this Paper, we provide details of the calculations in Ref. [2], and introduce three new families of laser models which may be considered as generalizations of those presented in that work. Each of these families of laser models is parameterized by a real number,  $p$ , with  $p = 4$  corresponding to the original models. The parameter space of these laser families is numerically investigated in detail, where we explore the influence of these parameters on both the coherence and photon statistics of the laser beams. Two distinct regimes for the coherence may be identified based on the choice of  $p$ , where for  $p > 3$ , each family of models exhibits Heisenberg-limited beam coherence, while for  $p < 3$ , the Heisenberg limit is no longer attained. Moreover, in the former regime, we derive formulae for the beam coherence of each of these three laser families which agree with the numerics. We find that the optimal parameter is in fact  $p \approx 4.15$ , not  $p = 4$ .

## I. INTRODUCTION

As the frontier of quantum technology enters the NISQ era, remarkable levels of control over quantum systems have been demonstrated [3, 4], bringing us to the point at which the properties of quantum mechanics are exploited to achieve feats that would be impractical by any classical device [5–11]. However, in striving towards the quantum technologies of the future and the powerful applications they potentially offer, it remains imperative that quantum scientists and engineers alike continue pushing the envelope of discovery towards the enhanced control over quantum systems [12].

Recent work regarding the limit to the amount of optical coherence that can be produced by a laser marks an example of this [1]. Coherence is a quantity that is of fundamental importance not only in the field of quantum technology [13, 14], but to precision technology in general [15]. In that work, the authors demonstrated that a quantum enhancement is possible for the coherence (a quantity that is reciprocally proportional to the linewidth,  $\ell$ , or phase diffusion rate) of a continuous wave (CW) laser. In this context, a quantum enhancement is said to exist if the ultimate limit imposed by quantum theory, or *Heisenberg limit*, for the performance of a device scales better in terms of a particular resource when compared to the standard quantum limit (SQL).

The principled definition in Ref. [1] of laser coherence,

denoted by  $\mathfrak{C}$ , implies that for ‘ideal’ laser beams, it is proportional to the product of the photon flux,  $\mathcal{N}$ , and the coherence time,  $1/\ell$ . The authors of [1] then derived the Heisenberg limit for a laser with such ‘ideal’ properties (see below),  $\mathfrak{C}_{\text{HL}}^{\text{ideal}} = \Theta(\mu^4)$ . Here,  $\mu$  is the mean number of photons within the laser, and is a critical resource for the production of a highly coherent beam of light. Thus, a quadratic enhancement over the Schawlow-Townes limit [17],  $\mathfrak{C}_{\text{SQL}}^{\text{ideal}} = \Theta(\mu^2)$ , was theoretically demonstrated, forcing one to adopt the notion that this historic limit is only a SQL, and could be far surpassed by the Heisenberg limit. Note that throughout this Paper we make use of Bachmann-Landau notation to describe the limiting behaviour of particular functions [16]; the  $\Theta$ -notation given above means that  $\mathfrak{C}_{\text{HL}}^{\text{ideal}}$ , for instance, is bounded both above and below by  $\mu^4$  asymptotically. Formally, this is to say that there exist two positive constants,  $k_1$  and  $k_2$ , and a  $\mu_0$ , such that, for all  $\mu > \mu_0$ , we have  $k_1\mu^4 \leq |\mathfrak{C}_{\text{HL}}^{\text{ideal}}(\mu)| \leq k_2\mu^4$ .

A model for a laser that produces a beam with Heisenberg-limited scaling of  $\mathfrak{C}$  was also put forward in that work. The key element in that model is that the input and output coupling are highly nonlinear, and a potential implementation on the platform of circuit-QED was given. Parallel to this, an independent group also demonstrated theoretically that the SQL for  $\mathfrak{C}$  can be surpassed via a different proposal with a circuit-QED architecture [18]. Like the former model, the key element in the design was that the input and output coupling of the laser to its environment contains a nonlinear component. The circuit proposed in [18] may be more practical than that in Ref. [1]. However, while it surpasses the SQL,

<sup>\*</sup> lucas.ostrowski@griffithuni.edu.au

<sup>†</sup> h.wiseman@griffith.edu.au

with  $\mathfrak{C} = \Theta(\mu^3)$  it does not achieve the Heisenberg limit.

In light of these recent theoretical results, the general focus of this Paper, along with our companion Letter [2], is to explore the restrictions (if any) that are placed on laser beams that exhibit Heisenberg-limited coherence given particular beam photon statistics. A natural question to ask here is if measures are taken to squeeze the number fluctuations in such a beam, would this come at the cost of a reduction in the coherence? While answering this query is the primary goal of our companion Letter [2], the motivation of this Paper is to flesh out many of the details that are omitted from that Letter for the sake of brevity. In an extension of this, we present a range of new results for three families of laser models that exhibit Heisenberg-limited coherence. These include a detailed exploration of the parameter spaces characterizing these families, and derivations of formulae for the coherence of the laser beams that agree with numerical calculations.

Details for the proof of Theorem 1 in Ref. [2] are provided here. This theorem demonstrates that that  $\mathfrak{C} = O(\mu^4)$  remains as the Heisenberg limit under relaxed conditions on the beam, which includes a more general class of lasers that do not rule out beams that can be highly sub-Poissonian. In turn, three families of laser models are introduced, which are shown to be within the class of models for which Theorem 1 holds and also exhibit Heisenberg-limited coherence with  $\mathfrak{C} = \Theta(\mu^4)$ . These three families may be considered as generalizations of those given in Ref. [2] and are conceived by making modifications to the gain and loss mechanisms between the laser and its surrounding environment from the original laser model of Ref. [1]. Each can be aptly distinguished from one another by considering only their pumping mechanisms: The first involves a *randomly pumped (Markovian), quasi-isometric gain*; the second involves a *randomly pumped, non-isometric gain*; and the third involves a *regularly pumped (non-Markovian), quasi-isometric gain*. For ease of reference, these will be referred to according to the key parameters that characterize them, being the *p-family*, the  *$\lambda, p$ -family* and the *q, p-family* of Heisenberg-limited laser models, respectively. Both of the last two of these are shown to exhibit sub-Poissonian beam photon statistics, and both reduce to the first family in the Poissonian limit.

With these generalizations, the aforementioned query regarding the trade-off between coherence and sub-Poissonianity is able to be addressed. We find that by imposing parameter values that maximise the coherence in these two families that can exhibit sub-Poissonian photons statistics in the beam (quantified by the Mandel-Q parameter), the degree of this sub-Poissonianity is also maximized. Moreover, the maximum coherence attained in these families is significantly larger than the original model presented in Ref. [1]. Therefore, by providing these two counterexamples, the conclusion is made that there is no trade-off between coherence and sub-Poissonianity for lasers with Heisenberg-limited coherence. On the con-

trary, it appears to be advantageous for the optimization of the coherence if measures are taken to reduce the number fluctuations in the beam.

An important new aspect of the three families of laser models mentioned above is the parameter  $p$ . This controls the variance of the steady-state laser cavity distribution and is shown to have a strong influence on the coherence, as two distinct regimes may be identified for each family with respect to this parameter. For values  $p \gtrsim 3$ , we find the scaling of the coherence for all families is  $\mathfrak{C} = \Theta(\mu^4)$ . That is to say that  $\mathfrak{C}$  is Heisenberg-limited within this regime. Moreover, we find that a peak in the coherence in this regime is found at  $p \approx 4.15$  for each family, slightly different from the value  $p = 4$  used in Refs. [1, 2]. On the other hand, for values  $p \lesssim 3$  (which means even broader cavity distributions), we find a change in exponent of the power law for the coherence and Heisenberg-limited scaling is lost. Here, we instead find the relationship between  $\mathfrak{C}$  and  $\mu$  to be approximately  $\mathfrak{C} = \Theta(\mu^{p+1})$ . We were able to reproduce all of this behaviour by heuristic arguments.

The remainder of this Paper is structured as follows. In Section II we introduce and discuss the key concepts and quantities of interest throughout this Paper: the coherence and sub-Poissonianity of a laser beam, and our adopted measures of them. The conditions we place on a laser and its beam to derive the Heisenberg limit for the coherence are also summarized here, and we outline the differences between these and that given in Ref. [1]. In Section III we derive the upper bound for  $\mathfrak{C}$  under these four conditions, which allows for beams that can be highly sub-Poissonian. In Section IV we briefly review the basic description of a laser in an iMPS framework and the numerical methods employed to compute the physical quantities of interest within this framework. In Section V we introduce the three families of laser models which will be the subject of analysis for the subsequent sections of the Paper. Section VI provides a numerical analysis of these three families of laser models, where we explore the parameter spaces characterizing each family in detail and identify interesting behaviour of the physical quantities which quantify the beam coherence and degree of beam sub-Poissonianity. In Section VII we provide an analysis of the coherence, where we are able to derive formulae for our three families of models in the “Heisenberg-limited regime” characterized by  $p > 3$ . We are able to show that these formulae accurately reproduce our numerical results given in Section VI and based on this analysis, we are able to provide arguments as to why Heisenberg-limited coherence is lost for  $p < 3$ . Finally, in Section VIII we summarize our results and provide some concluding remarks.

## II. LASERS, COHERENCE AND SUB-POISSONIANITY

### A. Laser Coherence

Consider a one-dimensional bosonic beam travelling at fixed speed with translationally invariant statistics, which can be described by the single-parameter field operator  $\hat{b}(t)$ . Our adopted measure of coherence for such a beam may be defined generally as the mean number of photons in the maximally populated spatial mode [1]. This amounts to the mathematical statement

$$\mathfrak{C} := \max_{u \in \mathbf{u}} \langle \hat{b}_u^\dagger \hat{b}_u \rangle, \quad (1)$$

where  $\hat{b}_u = (1/\sqrt{I_u}) \int_{-\infty}^{\infty} dt u(t) \hat{b}(t)$  defines the annihilation operator for mode  $u$ . Here,  $I_u = \int_{-\infty}^{\infty} dt |u(t)|^2$  is a normalization factor, while the maximization is over the modes  $\mathbf{u}$  within a particular frequency band; this avoids the trouble associated with a thermal state with arbitrarily low frequency having an exceedingly large coherence.

For a beam with translationally invariant statistics, the mode  $u$  which attains the maximum in Eq. (1) is characterised by a flat waveform. Strictly, such a mode is not in  $\mathbf{u}$  as it is not square integrable, but we can consider  $u_T(t) \propto e^{-|t|/T}$  and afterwards take the limit  $T \rightarrow \infty$ . Consequently,  $\mathfrak{C}$  is directly proportional to the maximum of the power spectrum [1], and as it is possible to redefine  $\hat{b}(t)$  so as to absorb the rotation at the spectral peak frequency, the coherence may be expressed as

$$\mathfrak{C} = \int_{-\infty}^{\infty} d\tau G^{(1)}(t, \tau). \quad (2)$$

Here the  $n^{\text{th}}$ -order Glauber coherence functions are defined in the usual way [22]

$$G^{(n)}(s_1, \dots, s_{2n}) := \langle \hat{b}^\dagger(s_1) \cdots \hat{b}^\dagger(s_n) \hat{b}(s_{n+1}) \cdots \hat{b}(s_{2n}) \rangle, \quad (3)$$

with corresponding normalized forms

$$g^{(n)}(s_1, \dots, s_{2n}) := \frac{\langle \hat{b}^\dagger(s_1) \cdots \hat{b}^\dagger(s_n) \hat{b}(s_{n+1}) \cdots \hat{b}(s_{2n}) \rangle}{\Pi_{i=1}^{2n} |G^{(1)}(s_i, s_i)|^{1/2}}. \quad (4)$$

With translationally invariant statistics, the denominator of Eq. (4) can be expressed as  $\Pi_{i=1}^{2n} |G^{(1)}(s_i, s_i)|^{1/2} = \mathcal{N}^n$ , where we define

$$\mathcal{N} := G^{(1)}(t, t). \quad (5)$$

This quantity is interpreted as the photon flux from the laser.

It is well-established that, far above threshold, the state produced by an ideal standard CW laser in the absence of any technical noise can be described by a coherent state undergoing pure phase diffusion [23–25]. That is, the beam can be described by an eigenstate

$$|\beta(t)\rangle = \left| \sqrt{\mathcal{N}} e^{i\sqrt{\ell} W(t)} \right\rangle, \quad (6)$$

of  $\hat{b}(t)$ , where  $W(t)$  represents a Wiener process. For such beams, the coherence may be evaluated in terms of  $\mathcal{N}$  and the full-width at half-maximum (FWHM) of its Lorentzian Power spectrum (or linewidth),  $\ell$ , as

$$\mathfrak{C} = \frac{4\mathcal{N}}{\ell}. \quad (7)$$

In this instance, we see that  $\mathfrak{C}$  has a straightforward interpretation, as roughly the number of photons that are emitted into the beam that are mutually coherent.

A noteworthy point regarding this measure of coherence is that it does not require an absolute phase or mean field, but is instead a statement of the beam's *relative coherence*. In fact, by considering the action on the field imposed by a beamsplitter [1], this coherence measure may be shown to be a monotonic function of the relative entropy of asymmetry [26], which is a well established coherence measure employed in quantum information theory [27, 28].

### B. Beam Photon Statistics

As we have already alluded to, a key concept within this Paper is with regard to sub-Poissonian light in the *output* field. The degree to which the output field is sub-Poissonian may be quantified by the Mandel-Q parameter defined over the time duration  $S$  [29, 30],

$$Q_S := \frac{\langle (\Delta \hat{n}_S)^2 \rangle - \langle \hat{n}_S \rangle}{\langle \hat{n}_S \rangle}, \quad (8)$$

where  $\hat{n}_S := \int_0^S ds \hat{b}^\dagger(s) \hat{b}(s)$  is the number operator for the beam over the interval  $[0, S]$ . This quantity may be interpreted as the normalised variance in the number of detections made by an ideal photodetector monitoring the beam over this time interval. For example,  $-1 \leq Q_S < 0$  would imply that the variance in photodetections made between successive measurements is less than the mean, which is the defining property of sub-Poissonian light.

For stationary fields, this quantity may be expressed in terms of the second-order Glauber coherence function [31, 32]

$$Q_S = \frac{\langle \hat{n}_S \rangle}{S^2} \int_{-S}^S d\tau (S - |\tau|) \left( g_{\text{ps}}^{(2)}(\tau) - 1 \right), \quad (9)$$

where  $g_{\text{ps}}^{(2)}(\tau) := g^{(2)}(t, t + \tau, t + \tau, t)$ . Here, the subscript ps stands for photon statistics. Expressing  $Q_S$  in this manner will be useful for calculations made in the following sections. Of particular interest to us is the long-time limit, where  $S \rightarrow \infty$ , as this is the counting duration that gives the smallest Q-parameter. We therefore drop the subscript for ease of notation, such that  $Q \equiv Q_{S \rightarrow \infty}$  and use this quantity as our measure of the degree of sub-Poissonianity in the laser beam.

### C. Conditions on the Laser and its Beam

In order to speak of the Heisenberg limit for the coherence of a CW laser beam, we must of course specify the constraints placed on the particular systems for which this limit applies. In Ref. [1], the constraints which led to the derivation of the Heisenberg-limit amounted to four conditions that were imposed on the laser and the beam it produces (note that we use the terms ‘laser’ and ‘laser cavity’ interchangeably here). Together, these conditions encapsulate the most fundamental aspects of the radiation that is produced from the laser models developed throughout the 1960’s and 70’s [23, 24, 33]. In addition to this, they also constrain the mechanism by which incoherent inputs to a laser are converted into a highly coherent output beam of radiation. The first three of these conditions will be adopted outright by us and we will not explain these in detail here as this has already been done at length in Ref. [1]. However, they may be summarized in the following way:

1. **One Dimensional Beam**—The beam propagates away from the laser in one direction at a constant speed, occupying a single transverse mode and polarisation. The beam can therefore be described by a scalar quantum field with the annihilation operator  $\hat{b}(t)$  satisfying  $[\hat{b}(t), \hat{b}^\dagger(t')] = \delta(t - t')$  (this was already used above).
2. **Endogenous Phase**—Coherence in the beam can only be proceed from excitations within the laser. That is, a phase shift imposed on the laser state at some time  $T$  will lead, in the future, to the same phase shift on the beam emitted after time  $T$ , as well as on the laser state.
3. **Stationary Beam Statistics**—The statistics of the laser and beam have a long-time limit that is unique and invariant under time translation. This means that the mean excitation number within the laser,  $\langle \hat{n}_c \rangle$ , has a unique stationary value  $\mu$ .

The fourth condition that we impose on the beam is similar to the “Ideal Glauber<sup>(1),(2)</sup>-coherence” condition of Ref. [1], albeit with some necessary modification. The “Ideal Glauber<sup>(1),(2)</sup>-coherence” condition stated that the first- and second-order coherence functions of Eq. (4) for a particular laser model is well-approximated by that of a coherent state undergoing pure phase diffusion (Eq. (6)). This was defined in this manner in order to derive the upper bound for  $\mathfrak{C}$ . The reason that we require this condition to be modified is because it rules out beams for which  $g^{(2)}(s, s', t', t)$  significantly deviates from that produced by a coherent state with a diffusing phase, therefore excluding beams which exhibit sub-Poissonian photon statistics. In order to not exclude such beams, the fourth condition that we impose on the beam is as follows:

4. **Passably Ideal Glauber Coherence**—The first- and second-order Glauber coherence functions are *passably close* to that produced by the state of an ideal laser, i.e, an eigenstate  $|\beta(t)\rangle$  of  $\hat{b}(t)$  with eigenvalue  $\beta(t) = \sqrt{\mathcal{N}}e^{i\sqrt{\mathfrak{C}}W(t)}$  and  $W(t)$  representing a Wiener process.

Here, the addition of “passably” in the above definition is to distinguish this condition from the original Condition 4. Explicitly, what we mean by our new Condition 4 is

$$|g_{\text{laser}}^{(1)}(s, t) - g_{\text{ideal}}^{(1)}(s, t)| = O(1), \quad (10a)$$

$$|g_{\text{laser}}^{(2)}(s, s', t', t) - g_{\text{ideal}}^{(2)}(s, s', t', t)| = O(\mathfrak{C}^{-1/2}), \quad (10b)$$

for all values of the time arguments such that the difference between any two times is  $O(\sqrt{\mathfrak{C}}/\mathcal{N})$ . Consideration of this time difference is to yield the tightest upper bound for the coherence of such a laser (see Theorem 1, below). The subscripts ‘ideal’ and ‘laser’ seen in Eqs. (10a) and (10b) denote the coherence functions pertaining to an ideal laser beam (i.e, that which is described exactly by Eq. (6)), and those for a specific laser model, respectively.

The difference between the current Condition 4 and the original one conceived in Ref. [1] is that the latter would replace  $O$  on the RHS of Eqs. (10a) and (10b) with  $o$ . With Bachmann–Landau notation,  $f(x) = o(g(x))$  formally means that for all positive constants,  $k$ , there exists an  $x_0$ , such that, for all  $x > x_0$ , then  $|f(x)| < kg(x)$ , while  $f(x) = O(g(x))$  instead means  $|f(x)| \leq kg(x)$ , with  $k$  and  $x$  specified in the same manner [16]. The former condition is thus a much stricter requirement on the beam. The most important implication of this change is that this updated condition permits  $g^{(2)}$  to deviate considerably from an ‘ideal’ laser beam, therefore including models with sub-Poissonian beam photon statistics. As we will see, this allows beams with corresponding values of  $Q$  arbitrarily close to the minimum of  $-1$  to satisfy these four conditions.

### III. THE HEISENBERG LIMIT FOR $\mathfrak{C}$

We now move on to present a proof of the upper bound for  $\mathfrak{C}$ , under the revised conditions discussed previously. This proof closely follows that for Theorem 1 in Ref. [1], with the difference here being that the proof is modified according to Eqs. (10a) and (10b), such that a more general Heisenberg limit for  $\mathfrak{C}$  is derived. Therefore, this limit encompasses laser models that exhibit highly sub-Poissonian beam statistics. A consequence of this generalisation is that an upper bound with a specific prefactor is no longer able to be obtained, only the scaling  $\mathfrak{C} = O(\mu^4)$ , which is nevertheless sufficient to talk of the Heisenberg limit. Since the proof of the following theorem bears a good deal of resemblance with that of Ref. [1], we only present the key details of the modifications made.



It is also worth noting that in what follows, we define the “linewidth” of a laser model satisfying the four conditions detailed in Section II C as

$$\ell := 4\mathcal{N}/\mathfrak{C}, \quad (11)$$

with  $\mathfrak{C}$  and  $\mathcal{N}$  respectively given by Eqs. (1) and (5). This does not necessarily imply that this quantity corresponds to the FWHM of a Lorentzian power spectrum as implied from the argument leading to Eq. (7). Rather, it allows a connection to be drawn between the FWHM of an ideal laser beam, defined by Eq. (6), and the coherence of laser model satisfying Conditions 1–4, which we set out to derive a bound for, from above.

**Theorem 1:** (Generalisation of the upper bound on  $\mathfrak{C}$  for sub-Poissonian lasers). *For a laser which satisfies conditions 1–4 stated above, the coherence is bounded from above:*

$$\mathfrak{C} = O(\mu^4), \quad (12)$$

where  $\mu$  is the mean number of excitations within the laser.

*Proof.* This involves an observer, Effie, to first perform a *filtering* heterodyne measurement on the beam over the time interval  $[T - \tau, T]$ . A second observer, Rod, is then tasked with estimating the optical phase,  $\phi_F$ , that is encoded on the cavity state at time  $T$  by Effie’s measurement. The methods that Rod considers to carry this out is to either make a *retrofiltering* heterodyne measurement on the beam over the time interval  $(T, T + \tau]$  to obtain the estimate  $\phi_R$ , or perform a direct cavity measurement to obtain the estimate  $\phi_D$ . As the result  $\phi_R$  cannot outperform  $\phi_D$  as an estimate of  $\phi_F$  [1], the upper bound on  $\mathfrak{C}$  will follow from known results on optimal covariant phase estimation.

We first consider Rod’s retrofiltering measurement. In order to describe the two heterodyne measurements in this problem, the unitary operators  $e^{i\hat{\phi}_R}$  and  $e^{i\hat{\phi}_F}$  are defined, which have unit-modulus complex eigenvalues and arguments that give the phase estimates  $\phi_F$  and  $\phi_R$  for the respective filtering and retrofiltering measurements.

These operators may be expressed as [34]

$$e^{i\hat{\phi}_F} = \hat{F}/\sqrt{\hat{F}^\dagger \hat{F}}, \quad (13a)$$

$$e^{i\hat{\phi}_R} = \hat{R}/\sqrt{\hat{R}^\dagger \hat{R}}, \quad (13b)$$

with

$$\hat{F} := \int_{T-\tau}^T dt u_F(t) \hat{b}(t) + \hat{a}_F^\dagger, \quad (14a)$$

$$\hat{R} := \int_T^{T+\tau} dt u_R(t) \hat{b}(t) + \hat{a}_R^\dagger. \quad (14b)$$

Here,  $\hat{a}_{F(R)}$  are annihilation operators for the ancillary vacuum modes that enters into heterodyne detection and  $u_{F(R)}$  are normalised filter functions, which, for simplicity, are taken as  $u_F(t) = u_R(-t) = \tau^{-1/2}[H(t) - H(t - \tau)]$ , where  $H(t)$  is the Heaviside step function.

An important result from Ref. [1] was to show that the observables  $e^{i\hat{\phi}_F}$  and  $e^{i\hat{\phi}_R}$  change covariantly when a phase shift of arbitrary angle is imposed on the beam. Consequently, for the laser in its unique steady-state  $\rho_{ss}$  (which has mean excitation number  $\mu$  and is invariant under arbitrary phase shifts), the cavity state conditioned on Effie’s measurement is equivalent to a fiducial cavity state,  $\rho_0$ , with an optical phase,  $\phi_F$ , encoded by the generator  $\hat{n}_c$  (the cavity photon number operator). Crucially, this conditioned state,  $\rho_{c|\phi_F} = e^{i\phi_F \hat{n}_c} \rho_0 e^{-i\phi_F \hat{n}_c}$ , has a mean excitation number  $\mu$  regardless of the measurement outcome  $\phi_F$ .

To compare how correlated Rod’s retrofiltering measurement  $\phi_R$  is with Effie’s result  $\phi_F$ , we consider the quantity  $1 - |\langle e^{i(\hat{\phi}_R - \hat{\phi}_F)} \rangle|^2$ . This provides a convenient measure of the phase spread by recognizing that, for small errors  $\theta$ ,  $1 - |\langle e^{i\theta} \rangle| \approx \langle \theta^2 \rangle - \langle \theta \rangle^2$  is the mean-square error (MSE) for an unbiased estimate of  $\theta$ . With the definitions outlined in Eqs. (13) and (14), it is possible to express this quantity as being asymptotically equivalent to an expression involving the first- and second-order Glauber coherence functions defined in Eqs. (3a) and (3b) [1]. That is, for  $\ell\tau \ll 1$  and  $\mathcal{N}\tau \gg 1$ , one has

$$1 - |\langle e^{i(\hat{\phi}_R - \hat{\phi}_F)} \rangle|^2 \sim \frac{1}{2\mathcal{N}^2\tau^2} + \frac{1}{\mathcal{N}\tau^3} \int_0^\tau dt \int_0^\tau ds g^{(1)}(s, t) + \frac{1}{2\tau^4} \left[ \int_0^\tau ds \int_{-\tau}^0 ds' \int_0^\tau dt' \int_{-\tau}^0 dt g^{(2)}(s, s', t', t) - \int_0^\tau ds \int_0^\tau ds' \int_{-\tau}^0 dt' \int_{-\tau}^0 dt g^{(2)}(s, s', t', t) \right]. \quad (15)$$

It is straightforward to evaluate Eq. (15) for an ideal laser

described by the state  $|\beta(t)\rangle$ , as defined in Eq. (6). To

leading order in  $\ell/\mathcal{N}$ , We find

$$1 - |\langle e^{i(\hat{\phi}_R - \hat{\phi}_F)} \rangle|_{\text{ideal}}^2 \sim 2\sqrt{\frac{2\ell}{3\mathcal{N}}}. \quad (16)$$

To arrive at this expression we have chosen  $\tau = \sqrt{\frac{3}{2}}\mathfrak{C}/\mathcal{N}$ , as this choice for the time interval minimizes the error in the retrofiltering measurement. This is done such that the tightest possible bound for the coherence is obtained from this method. It is worth noting that while this prefactor of  $\sqrt{3/2}$  has been included for completeness here, it is irrelevant for the purposes of this proof. In fact, one could just as well set  $\tau = \Theta(\sqrt{\mathfrak{C}/\mathcal{N}})$  and arrive at the same result. This is because, unlike Theorem 1 of Ref. [1], we are concerned only with the scaling of the upper bound for  $\mathfrak{C}$ , rather than obtaining a specific prefactor.

If one now considers a general laser model that satisfies Conditions 1–4, it may be seen from Equations (15) and (16) that the *relative* difference,  $\Delta$ , in the MSE, between this model and an ideal laser for the retrofiltering measurement, can be bounded above:

$$\Delta = O\left(\max_{s,t \in [0,\tau]} |\delta g^{(1)}(s,t)|\right) + O\left(\sqrt{\mathcal{N}/\ell} \max_{s,s',t',t \in [-\tau,\tau]} |\delta g^{(2)}(s,s',t',t)|\right), \quad (17)$$

where

$$\delta g^{(n)}(s_1, \dots, s_{2n}) := g_{\text{laser}}^{(n)}(s_1, \dots, s_{2n}) - g_{\text{ideal}}^{(n)}(s_1, \dots, s_{2n}). \quad (18)$$

From here we may write down an expression for an upper bound on the MSE from a retrofiltering measurement for this family of laser models,

$$1 - |\langle e^{i(\hat{\phi}_R - \hat{\phi}_F)} \rangle|_{\text{laser}}^2 \leq 2\sqrt{\frac{2\ell}{3\mathcal{N}}} (1 + |\Delta|). \quad (19)$$

Invoking Condition 4, the relative difference  $\Delta$  becomes  $O(1)$ , and the RHS of Eq. (19) becomes  $O(\sqrt{\ell/\mathcal{N}})$ . Rewriting this in terms of the coherence, from Eq. (11), we have

$$1 - |\langle e^{i(\hat{\phi}_R - \hat{\phi}_F)} \rangle|_{\text{laser}}^2 = O(\mathfrak{C}^{-1/2}). \quad (20)$$

It is now possible to obtain a bound for  $\mathfrak{C}$  in terms of  $\mu$  by considering the fact that it is impossible for a phase estimate of  $\phi_F$  obtained from a heterodyne measurement to outperform an estimate  $\phi_D$  obtained through a direct cavity measurement, i.e.,

$$1 - |\langle e^{i(\hat{\phi}_R - \hat{\phi}_F)} \rangle|^2 \geq 1 - |\langle e^{i(\hat{\phi}_D - \hat{\phi}_F)} \rangle|^2. \quad (21)$$

This is guaranteed by imposing Conditions 1–3 [1]. It is a known result that the error in an estimate of the cavity phase obtained from a direct cavity measurement can be bounded from below [35],

$$1 - |\langle e^{i(\hat{\phi}_D - \hat{\phi}_F)} \rangle|^2 = \Omega(\mu^{-2}), \quad (22)$$

where we are again making use of Bachmann–Landau notation, with  $f(x) = \Omega(g(x))$  formally meaning that there exists a positive constant,  $k$ , and an  $x_0$ , such that, for all  $x > x_0$ , we have  $|f(x)| \geq kg(x)$ . Bringing together Eqs. (20), (21) and (22), an upper bound on  $\mathfrak{C}$  for any laser satisfying the stated conditions is readily obtained

$$\mathfrak{C} = O(\mu^4). \quad (23)$$

□

It will be demonstrated numerically that  $\mathfrak{C} \propto \mu^4$  for specific families of laser models considered in this Paper. Asserting that this scaling is indeed at the Heisenberg limit, Eqs. (10a) and (10b) are required to be verified; this is also to be shown numerically.

#### IV. NUMERICAL METHODS

Calculating the observable quantities of interest, namely the coherence and  $Q$ -parameter, for the laser models that we are to introduce, requires the evaluation of correlation functions of the beam. Given the large size of the Hilbert space of these systems, evaluating such functions using standard numerical methods is a computationally expensive task. We use infinite Matrix product state (iMPS) techniques that have been developed over recent decades, which make simulating large systems more tractable by providing efficient ways of describing the entanglement content of the wavefunction (see, e.g., Refs. [36, 37] for reviews). In this section we briefly review the treatment of a laser in the context of an MPS sequential quantum factory [38, 39], which is outlined in detail in Ref. [1], and discuss how particular physical quantities are calculated within this framework.

##### A. iMPS of a Laser Beam

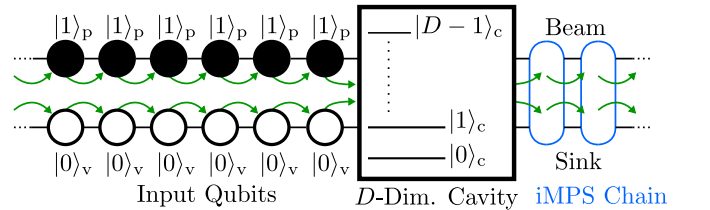


FIG. 1. Basic schematic of the laser model applicable to the  $p$ - and  $\lambda$ -families. A  $D$ -level cavity converts a pair of input qubits (pump and vacuum) into a pair of output qubits (beam and sink) at each time step of duration  $\delta t$ . Green arrows indicate the movement of the input and output qubits from one time-step to the next. The chain of output qubits, of indefinite length, is described by an iMPS with bond dimension  $D$ , equal to the Hilbert space dimension of the laser cavity.

In order to describe a laser beam in an iMPS framework, it is necessary to discretize the laser process by which incoherent excitations pumped into a cavity are converted into coherent excitations within the output beam. To this end, we consider the most basic form of a laser system as shown in Fig. 1, which consists of five elements that are all essential for operation: a “cavity” (c), pump (p), vacuum input (v), beam (b) and sink (s). In this model of a laser, the pump and vacuum inputs may be considered as a stream of incoming qubits into the cavity, which itself is treated as a  $D$ -level system with the non-degenerate number operator  $\hat{n}_c = \sum_{n=0}^{D-1} n|n\rangle_c \langle n|$ . The beam and sink are taken as a joint 4-level system (o), such that the laser consists of a single output in alignment with the requirements of an MPS sequential generation scheme. Addressing the beam alone is thus achieved by tracing over the sink. In this discretized approximation, a single beam qubit corresponds to an arbitrarily short beam segment of duration  $\delta t$ , such that it is occupied by at most one photon, where the bosonic operator for the beam is transformed as  $\sqrt{\delta t} \hat{b} \rightarrow \sigma_b^-$ , with  $\sigma_b^- = |1\rangle_b \langle 0|$ .

This discretized time evolution of the cavity and its outputs is governed by the generative interaction

$$\hat{V}_q = \sum_{j_{q+1}, m, n} A_{mn}^{[j_{q+1}]} |m\rangle_c \langle n| \otimes |j_{q+1}\rangle_o, \quad (24)$$

where  $|j_{q+1}\rangle_o := |j/2\rangle_{q+1} \otimes |(j \bmod 2)\rangle_s$  is defined on the output space. This generative interaction corresponds to an isometry (a purity-preserving, completely-positive, trace-preserving map) from a  $D$ -dimensional vector space to a  $4 \times D$ -dimensional one. It can be related to a generative unitary interaction,  $\hat{U}_{\text{int}}$ , according to  $\hat{V}|\psi\rangle_c \equiv \hat{U}_{\text{int}}(|\psi\rangle_c |1\rangle_p |0\rangle_v)$ . The isometry condition,  $\hat{V}^\dagger \hat{V} = I_D$ , with  $I_m$  as the  $m \times m$  identity matrix, translates to a completeness orthonormality relation

$$\sum_{j=0}^3 A^{[j]\dagger} A^{[j]} = I_D. \quad (25)$$

Of particular interest to us is the *one-site unit-cell* infinite MPS (iMPS) that  $\hat{V}$  eventually creates. In terms of the  $A$  matrices, this is given by

$$|\Psi_{\text{MPS}}\rangle = \sum_{\dots, j_{q_0}, j_{q_0-1}, j_{q_0-2}, \dots} \langle \Phi(q = +\infty) |_c \dots A_{(q_0)}^{[j_{q_0}]} A_{(q_0-1)}^{[j_{q_0-1}]} A_{(q_0-2)}^{[j_{q_0-2}]} \dots |\Phi(q = -\infty)\rangle_c |\dots, j_{q_0}, j_{q_0-1}, j_{q_0-2}, \dots\rangle. \quad (26)$$

Here,  $|\Phi(q)\rangle$  represents the state of the cavity at the discrete time  $q$  and it is assumed that in the last step  $q = +\infty$  the cavity decouples from the output. The  $(q_i)$ -subscripts shown above may also be dropped, which is permitted given that the outputs are translationally invariant. It is the case for all of our laser models that the largest-magnitude eigenvalue of the iMPS identity transfer matrix in its *flattened space*,  $\mathcal{T} = \sum_{j=0}^3 A^{[j]*} \otimes A^{[j]}$ , is

non-degenerate. This ensures that a unique steady state of the cavity exists and additionally renders the boundary states,  $|\Phi(q = \pm\infty)\rangle_c$ , to be irrelevant, in the sense that they will not appear in any calculations of the correlation functions. We also impose conservation of energy on the unitary  $\hat{U}_{\text{int}}$ , i.e.  $\hat{n}_c + \hat{n}_v + \hat{n}_p = \hat{n}'_c + \hat{n}'_v + \hat{n}'_p$  (with primes denoting the operators following the application of  $\hat{U}_{\text{int}}$ ). In doing so, we ensure that Condition 2 is satisfied, which requires that all phase information imprinted on the beam proceeds only from the laser cavity [1]. This results in the  $D \times D$  dimension  $A$ -matrices being highly sparse, where each matrix has at most a single non-zero diagonal, with  $O(D)$  free parameters. For each matrix, these non-zero elements correspond to the entries  $A_{m+1,m}^{[0]}$ ,  $A_{m,m}^{[1]}$ ,  $A_{m,m}^{[2]}$  and  $A_{m,m+1}^{[3]}$ , and are taken to be real and non-negative, consistent with a spectral peak at  $\omega = 0$ .

These  $A$ -matrices have clear physical interpretations:  $A^{[0]}$  describes the gain process into the cavity, relating to the amplitude of the cavity receiving an uncorrelated photon from the pump without emitting a photon to the output.  $A^{[1]}$  and  $A^{[2]}$  relate to the amplitude of the process where the cavity receives a pump photon and sends it directly into the sink and beam, respectively.  $A^{[2]}$  is therefore set to zero, as the photons emitted into the beam by this process add noise instead of contributing to the beam's coherence, therefore  $A^{[1]} = \sqrt{I_D - A^{[0]\dagger} A^{[0]} - A^{[3]\dagger} A^{[3]}}$  in accordance with Eq. (25). Finally,  $A^{[3]}$  describes the process of laser loss, which creates the beam, and relates to the amplitude of the cavity receiving an uncorrelated pump photon and emitting a single photon to both the beam and the sink, de-exciting the cavity by a single level.

It is possible to draw a connection between the laser dynamics in the framework presented above and that of a more traditional framework using a master equation for the cavity state,  $\dot{\rho} = \mathcal{L}\rho$ . This may be seen by considering the cavity state evolved by a single timestep  $\delta t$  in the iMPS framework,

$$\rho(t + \delta t) = \sum_j A^{[j]} \rho(t) A^{[j]\dagger}. \quad (27)$$

By taking the length of this discrete time interval to be infinitesimal,  $\delta t \rightarrow 0^+$ , a master equation is obtained with the Liouvillian,  $\mathcal{L}$ , taking the form

$$\begin{aligned} \frac{d\rho}{dt} &= \mathcal{L}\rho \\ &= \mathcal{N} \left( \mathcal{D}[\hat{G}] + \mathcal{D}[\hat{L}] \right) \rho, \end{aligned} \quad (28)$$

where  $\mathcal{D}[\hat{c}] := \hat{c} \bullet \hat{c}^\dagger - \frac{1}{2}(\hat{c}^\dagger \hat{c} \bullet + \bullet \hat{c}^\dagger \hat{c})$  is the usual Lindblad superoperator, and  $\hat{G}$  and  $\hat{L}$  are “gain” and “loss” operators, respectively, which specify how energy is added and released from the cavity. These gain and loss operators directly correspond to the iMPS operators  $B^{[0]} := A^{[0]}/\sqrt{\gamma}$  and  $B^{[3]} := A^{[3]}/\sqrt{\gamma}$ , respectively, with  $\gamma = \mathcal{N}\delta t$ . Explicit forms of these are given in the following Section.

## B. iMPS Calculations of $\mathfrak{C}$ , $Q$ and Glauber<sup>(1),(2)</sup> Correlators

For the discretized laser model introduced above, calculating the coherence amounts to evaluating the quantity

$$\mathfrak{C} = \sum_{q'=-\infty}^{\infty} \langle \sigma_b^+(q+q') \sigma_b^-(q) \rangle. \quad (29)$$

The method that is employed here to achieve this, as well as the calculation of the first- and second-order Glauber correlation functions, is the well-established method of manipulating MPS transfer operators [36]. In Ref. [1] it was demonstrated that, from this method, Eq. (29) may be re-expressed as

$$\mathfrak{C} = -2(1|(B^{[3]*} \otimes I_D) \cdot \text{inv}(\mathbb{Q}\mathbb{L}\mathbb{Q}) \cdot (I_D \otimes B^{[3]}|1), \quad (30)$$

which is written in *flattened space*, where superoperators such as the transfer-type operators become  $D^2 \times D^2$ -sized matrices and  $D \times D$ -sized operators are transformed into flattened  $D^2$ -sized vectors. Under this notation,  $\text{inv}(\bullet)$  represents the matrix inverse operation,  $|1\rangle \leftrightarrow I_D$  and  $|1\rangle \leftrightarrow \rho_{ss}$  are the left- and right-leading eigenvectors of  $\mathcal{T}$ , both of which have their eigenvalues equal to unity. This implies that the latter eigenvector satisfies the steady-state equation  $\sum_j \hat{A}^{[j]} \rho_{ss} \hat{A}^{[j]\dagger} = \rho_{ss}$ . Finally,  $\mathbb{Q} = I_{D^2} - |1\rangle\langle 1|$ , and  $\mathbb{L}$  represents the flattened space version of the superoperator defined in Eq. (28).

A simplified expression for the  $Q$ -parameter may also be found in terms of this flattened space iMPS language. Starting from Eq. (9),  $Q$  may be re-expressed as

$$Q = 2\gamma(1|(B^{[3]*} \otimes B^{[3]}) \cdot \text{inv}(I_{D^2} - \mathbb{Q}\mathcal{T}\mathbb{Q}) \cdot (B^{[3]*} \otimes B^{[3]}|1). \quad (31)$$

Additionally, the first- and second-order Glauber coherence functions are

$$G^{(1)}(s, 0) = (1|(B^{[3]*} \otimes I_D)\mathbb{E}(s)(I_D \otimes B^{[3]}|1), \quad (32a)$$

$$G^{(2)}(s, s', t', t) = (1|(B^{[3]*} \otimes I_D)\mathbb{E}(s' - s)(B^{[3]*} \otimes I_D) \mathbb{E}(t' - s')(I_D \otimes B^{[3]})\mathbb{E}(t - t')(I_D \otimes B^{[3]}|1), \quad (32b)$$

where  $\mathbb{E}(t) := \exp\{\mathcal{N}t\mathbb{L}\}$ . It is also worth noting that Eq. (32b) is for the specific time ordering  $s < s' < t' < t$ , but other time orderings may be calculated in a similar manner following an appropriate permutation of the bosonic operators. Eqs. (32a) and (32b) will be of use when verifying that our laser models satisfy Condition 4, details of which are given in Appendix B.

## V. FAMILIES OF LASER MODELS

### A. Quasi-Isometric, Markovian Gain ( $p$ -family)

In this section, we introduce three families of laser models, each of which will be shown to demonstrate Heisenberg-limited scaling of  $\mathfrak{C}$  for some range of parameter values. The first family may be characterized by the master equation

$$\begin{aligned} \frac{d\rho}{dt} &= \mathcal{L}_M^{(p,0)} \rho \\ &= \mathcal{N} \left( \mathcal{D}[\hat{G}^{(p,0)}] + \mathcal{D}[\hat{L}^{(p,0)}] \right) \rho, \end{aligned} \quad (33)$$

describing the evolution of a  $D$ -level cavity introduced above. Here, the subscript “M” in the Liouvillian superoperator stands for “Markov”,  $p \in (0, \infty)$ , and the non-zero elements of the gain and loss operators are defined generally as

$$G_n^{(p,x)} \propto \left( \frac{\sin\left(\pi \frac{n+1}{D+1}\right)}{\sin\left(\pi \frac{n}{D+1}\right)} \right)^{\frac{px}{2}}, \quad (34a)$$

$$L_n^{(p,x)} \propto \left( \frac{\sin\left(\pi \frac{n}{D+1}\right)}{\sin\left(\pi \frac{n+1}{D+1}\right)} \right)^{\frac{p(1-x)}{2}}, \quad (34b)$$

which are expressed here in the number basis of the cavity for  $(0 < n < D)$ , where

$$G_n^{(p,x)} \equiv \langle n | \hat{G}^{(p,x)} | n-1 \rangle, \quad L_n^{(p,x)} \equiv \langle n-1 | \hat{L}^{(p,x)} | n \rangle. \quad (35)$$

The parameter  $x$  in Eqs. (34a–b) can be any real number; however, for the case at hand we set  $x = 0$  therefore imposing a “flat” gain operator with  $\hat{G}_n^{(p,0)} \propto 1$ .

For this Master Equation (33), the steady state-cavity photon distribution may be found with  $\rho_n = |G_n^{(p,x)} / L_n^{(p,x)}|^2 \rho_{n-1}$ , such that

$$\rho_n = \alpha \sin^p \left( \pi \frac{n+1}{D+1} \right), \quad (0 \leq n < D), \quad (36)$$

where  $\rho_n = \langle n | \rho_{ss} | n \rangle$  and  $\mathcal{L}_M^{(p,0)} \rho_{ss} = 0$ . For this distribution, the mean photon number is  $\mu = (D-1)/2$  and in the asymptotic limit, as  $D \rightarrow \infty$ , the normalization factor has a straightforward expression,

$$\lim_{D \rightarrow \infty} D\alpha = \sqrt{\pi} \frac{\Gamma\left(\frac{2+p}{2}\right)}{\Gamma\left(\frac{1+p}{2}\right)}. \quad (37)$$

This family of laser models, defined by Eqs. (33) and (34), is a generalisation of the original laser model that exhibited Heisenberg-Limited coherence. That model was found via an optimization



of the iMPS  $A$ -matrices to maximize  $\mathfrak{C}$ , for  $D$  finite, which suggested the Ansatz (36) with  $p = 4$  [1]. This value of  $p$  was also used in the companion Letter [2] for the two families of models discussed below. In introducing this additional parameter,  $p$ , we are now able to modify the variance of the steady-state cavity distribution and thus explore the implications of this on the various physical properties of the system. Comparing this with the two other families of models that are to be introduced, we may distinguish this one by taking note of the gain process into the laser. In this situation, we identify this family as having a *quasi-isometric, Markovian* gain. Recalling that an isometric operator,  $\hat{V}$ , requires  $\hat{V}^\dagger \hat{V} = \hat{I}_D$ , we deem the use of the term “*quasi-isometric*” to be appropriate because  $\hat{G}^{(p,0)\dagger} \hat{G}^{(p,0)} = \hat{I}_D - \hat{\Pi}_{\text{top}}$ , where  $\hat{\Pi}_{\text{top}}$  is the projector onto the upper-most cavity state,

$$\hat{\Pi}_{\text{top}} \equiv |D-1\rangle\langle D-1|. \quad (38)$$

Therefore, in taking the limit where the dimension of the Hilbert space of the cavity tends to infinity,  $\hat{G}^{(p,0)}$  is approximately isometric for the particular types of states we concern ourselves with in this work. That is, for states with negligible population in the upper-most cavity state in this large- $D$  limit. This point is addressed in more detail in Appendix A. Throughout this Paper, this family of laser models will be referred to as the  $p$ -family.

### B. Non-Isometric, Markovian Gain ( $p, \lambda$ -family)

The second family of laser models we introduce may also be characterized by a master equation in the form of Eq. (28), with the Liouvillian  $\mathcal{L}_M^{(p,\lambda)}$ , such that

$$\begin{aligned} \frac{d\rho}{dt} &= \mathcal{L}_M^{(p,\lambda)} \rho \\ &= \mathcal{N} \left( \mathcal{D}[\hat{G}^{(p,\lambda)}] + \mathcal{D}[\hat{L}^{(p,\lambda)}] \right) \rho. \end{aligned} \quad (39)$$

Evidently, in addition to  $p$ , we have introduced another continuous parameter, with  $x \rightarrow \lambda \in \mathbb{R}$ , which allows for a significant modification to the form of the gain and loss operators of the system, while preserving the steady-state cavity distribution given in Eq. (36). Although  $\lambda$  may take any value within the set of real numbers, of particular interest to us are values falling within the range  $0 \leq \lambda \leq 1$ . Here, one may interchange smoothly between a flat gain operator, with  $\lambda \rightarrow 0.0$ , to a flat loss, with  $\lambda \rightarrow 1.0$ . This relationship between  $\lambda$  and the gain and loss operators is depicted in Fig. 2a–c, while the influence of  $p$  on the cavity distribution may be seen in in Fig. 2d. As will be shown both numerically and from heuristic arguments, modification of the gain and loss operators in this manner will have notable implications on both the coherence and photon statistics of the system. This family of laser models, exhibiting in general a *non-isometric*

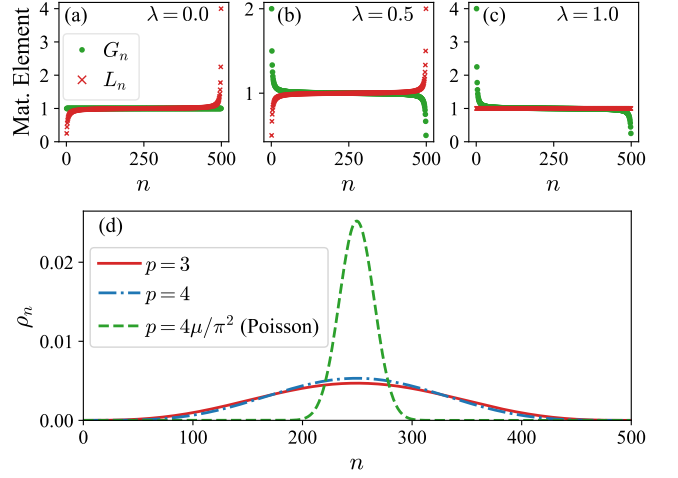


FIG. 2. (a–c) Non-zero matrix elements of the gain (green dots) and loss (red crosses) operators for the laser family exhibiting a non-isometric, Markovian gain model (i.e., the  $p, \lambda$ -family), for various choices of  $\lambda$  and cavity dimension  $D = 500$ . (d) Steady-state cavity photon distribution of the three laser families (36) for  $p = 3$  (solid red line),  $p = 4$  (blue dashed-dotted line) and  $p = 4\mu/\pi^2$  (green dashed line), with cavity dimension  $D = 500$ . Optimal coherence is obtained in each family of models for  $p \approx 4.15$ .

( $\hat{G}^{(p,\lambda)\dagger} \hat{G}^{(p,\lambda)} \approx \hat{I}_D$  for  $\lambda \neq 0$ ), *Markovian* gain mechanism, will be referred to as the  $p, \lambda$ -family according to the two key parameters which characterize it.

### C. Quasi-Isometric, Non-Markovian Gain ( $p, q$ -family)

For the  $p, \lambda$ -family introduced above, we will demonstrate that the beam exhibits sub-Poissonian photon statistics under particular choices of parameter, but the maximum attainable reduction in photon noise in the output field (that is,  $Q = -1$ ) is not achieved within this family. However, it is possible for complete noise reduction to be attained, at least in principle, for laser systems by introducing a mechanism by which the pumping of excitations into the cavity is done so in a regular manner [40–44]. The basic idea behind this can be understood simply by a consideration of particle number conservation. That is, if every pumped excitation will sooner or later be emitted as a photon into the beam, then the long-time photon statistics of the output field will mirror that of the pumping mechanism. Hence, for a completely regular pump, complete photon noise reduction would be possible in the output field for long counting intervals [41, 42].

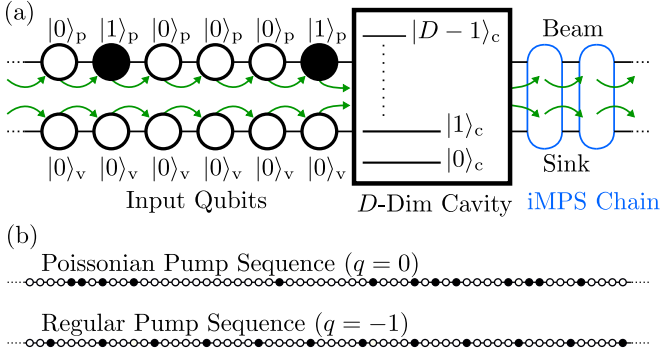


FIG. 3. (a) Basic schematic of the laser model applicable to the  $p, q$ -family. The elements of this model are much the same as that of Fig. 1. However, in this situation, the pumping sequence has been altered in order to facilitate the process by which pump excitations are deposited in the laser cavity in a regular manner. (b) Qualitative depictions of particular examples of pumping sequences. Top row shows the pumping sequence for the choice of parameter  $q = 0.0$ , where the number of excitations absorbed by the cavity in some time  $\Delta t$  is sampled from a Poisson distribution. Bottom row shows the pumping sequence where the entry of excitations into the cavity are made to be perfectly regular by choosing  $q = -1.0$ . Here, there is no variance in the number of excitations absorbed by the cavity in the time  $\Delta t$ .

Over the years a number of models have been proposed which can achieve this. For example, by making modifications to the Scully and Lamb theory [45] to account for a regular stream of excited atoms into the laser cavity (see, e.g., Ref. [46]). Similar effects can be achieved through internal mechanisms by which pump electrons are recycled through a number of rate-matched energy levels [47, 48]. To conclude this section we derive a master equation for a laser which incorporates a regular pumping mechanism, with the goal of producing a family of models that exhibit both Heisenberg-limited coherence, as well as complete photon noise reduction in the output field for long counting intervals for a specific choice of parameter. Our derivation follows closely to that given in Ref. [44], which is in the spirit of the generalisations made to the Scully Lamb model. The basic aim here is to incorporate a continuous parameter into the model that allows for the interchange between a Poissonian and regular injection of excitations into the  $D$ -level laser cavity mentioned above.

In order to aptly model this process within an iMPS framework, modifications must necessarily be made to the laser model introduced in the previous section. This modified system is depicted in Fig. 3a. Comparing this with Fig. 1, the most notable change is that that the pump qubits are no longer exclusively in the excited  $|1\rangle_p$  state. Although this is the case, this scenario represents a much more energy efficient process as it is formulated in such a way so that essentially every excited pump qubit will be converted into an excitation within the cavity. In particular, we define two unitary operators,  $\hat{U}_{\text{loss}}$  and  $\hat{U}_{\text{gain}}$ , which evolve system by a single timestep,  $\delta t$ , given

that the pump qubit is in the state  $|0\rangle_p$  or  $|1\rangle_p$ , respectively. Like the generative unitary interaction for the previous iMPS laser model, these two unitary operators map the  $4 \times D$ -dimensional vector space consisting of the pump and vacuum input qubits, and the cavity, to a  $4 \times D$ -dimensional one corresponding to the beam and sink generated by the cavity in  $\delta t$ , along with the evolved cavity state.

Explicitly, these operators are

$$\hat{U}_{\text{loss}} = \exp \left\{ \sqrt{\gamma} \left( \hat{L}^{(p, -q/2)} \otimes \hat{I}_p \otimes \hat{\sigma}_v^+ - \hat{L}^{\dagger(p, -q/2)} \otimes \hat{I}_p \otimes \hat{\sigma}_v^- \right) \right\}, \quad (40a)$$

$$\begin{aligned} \hat{U}_{\text{gain}} = & \hat{G}^{(p, 0)} \otimes \hat{\sigma}_p^- \otimes \hat{I}_v + \hat{G}^{\dagger(p, 0)} \otimes \hat{\sigma}_p^+ \otimes \hat{I}_v \\ & + \hat{\Pi}_{\text{top}} \otimes |1\rangle_p \langle 1| \otimes \hat{I}_v + \hat{\Pi}_{\text{bot}} \otimes |0\rangle_p \langle 0| \otimes \hat{I}_v. \end{aligned} \quad (40b)$$

Here,  $\hat{I}_p$  and  $\hat{I}_v$  are  $2 \times 2$  identity matrices acting on the space of the input pump and vacuum qubits, respectively.  $\hat{\Pi}_{\text{bot}}$  is the projector onto the ground state of the cavity,  $|0\rangle_c$ . The non-zero elements of the gain and loss operators ( $\hat{G}_n^{(p, 0)}$  and  $\hat{L}_n^{(p, -q/2)}$ ) are the same as those given in Eq. (34a–b), where we set  $x \rightarrow 0$  and  $x \rightarrow -q/2 \in (-\infty, 1/2)$ , respectively. Defining  $\hat{G}_n^{(p, 0)}$  in this manner ensures that the process of gain into the cavity corresponds to a completely-positive, trace-preserving operation, while  $\hat{L}_n^{(p, -q/2)}$  is defined in this manner to preserve the steady-state cavity distribution (36) (see Appendix A for details).

Considering generally a mixed cavity state,  $\rho(t)$ , the action of each of these gain and loss unitary operators lead to the incrementally evolved states

$$\rho_{\text{loss}}(t + \delta t) = (1 + \gamma \mathcal{D}[\hat{L}^{(p, -q/2)}])\rho(t), \quad (41a)$$

$$\rho_{\text{gain}}(t + \delta t) = (1 + (\mathcal{G} - 1))\rho(t), \quad (41b)$$

respectively, where  $\mathcal{G} \bullet = \hat{G}^{(p, 0)} \bullet \hat{G}^{\dagger(p, 0)} + \hat{\Pi}_{\text{top}} \bullet \hat{\Pi}_{\text{top}}$ . To arrive at these equations, we have traced over the beam and sink, as well as neglected terms of order  $O(\gamma^{3/2})$  and higher.

From here, we are in a position to incorporate pumping statistics which differ from the standard Poissonian case. To this end, we consider a short time,  $\Delta t$ , such that a large number,  $n(\Delta t)$ , of pump excitations have entered the cavity. Let us express this quantity in the following way

$$n(\Delta t) = \mathcal{N}\Delta t + \sqrt{\mathcal{N}(q+1)}\Delta W, \quad (42)$$

where  $\Delta W$  represents a Wiener increment [44] and  $q$  is the Mandel-Q parameter of the gain process. That is,  $q \rightarrow 0$  corresponds to a Poissonian process and  $q \rightarrow -1.0$  corresponds to a completely regular process (see Fig 3b for a depiction of each of these scenarios). The change

to the cavity state as a result of the gain process in this time is then given by

$$\rho_{\text{gain}}(t + \Delta t) = \left(1 + \mathcal{D}[\hat{G}^{(p,0)}] + \mathcal{D}[\hat{\Pi}_{\text{top}}]\right)^{n(\Delta t)} \rho(t). \quad (43)$$

Here, we are treating the gain and loss processes independently. This is justified under the assumption that  $1 \ll \mathcal{N}\Delta t \ll D$ , as the action of the superoperators  $\mathcal{D}[\hat{L}^{(p,-q/2)}]$  and  $(\mathcal{G} - 1)$  on the particular cavity states we consider in this work are of order  $O(D^{-1})$ . Details regarding this assumption may be found in Appendix A. Furthermore, given that the action of these superoperators is small, a binomial expansion of Eq. (43) is permitted, which, to second order in  $(\mathcal{G} - 1)$ , is

$$\begin{aligned} \rho_{\text{gain}}(t + \Delta t) \approx & [1 + n(\Delta t)(\mathcal{G} - 1) \\ & + (1/2)n(\Delta t)(n(\Delta t) - 1)(\mathcal{G} - 1)^2] \rho(t). \end{aligned} \quad (44)$$

Averaging over the uncertainty in the number of excitations added to the cavity and taking the limit  $\Delta t \rightarrow 0^+$ , one obtains the master equation

$$\begin{aligned} \frac{d\rho}{dt} = & \mathcal{L}_{\text{NM}}^{(p,q)} \rho \\ = & \mathcal{N} \left( \mathcal{D}[\hat{G}^{(p,0)}] + \frac{q}{2} \mathcal{D}[\hat{G}^{(p,0)}]^2 + \mathcal{D}[\hat{L}^{(p,-q/2)}] \right) \rho, \end{aligned} \quad (45)$$

where we have also reinstated the loss term,  $\mathcal{D}[\hat{L}^{(p,-q/2)}]$ . Here, the subscript “NM” stands for “Non-Markovian”. In order to maintain consistency with Eq. (33), such that Eq. (45) reduces to the master equation for the  $p$ -family for  $q \rightarrow 0$ , we have also let  $(\mathcal{G} - 1) \approx \mathcal{D}[\hat{G}^{(p,0)}]$ . Strictly speaking, one should have  $(\mathcal{G} - 1) = \mathcal{D}[\hat{G}^{(p,0)}] + \mathcal{D}[\hat{\Pi}_{\text{top}}]$ , however, though this neglected term is significant in general, it may be ignored by considering the same argument as before. That is, because the edge elements for the class of states considered in this study are negligible, the contribution of  $\mathcal{D}[\hat{\Pi}_{\text{top}}]$  in Eq. (45) will also be negligible. The reader is again referred to Appendix A for details.

Equation (45) is not in Lindblad form and thus it is only an approximate description of a regularly pumped laser. However, equations of the same form as this have commonly been employed in laser theory [40, 42, 44, 46, 49] and we will indeed show that reasonable results are obtained from our subsequent analysis. This family of laser models can be thought of exhibiting a *quasi-isometric, non-Markovian* gain mechanism. In line with our notation for the other two families of laser models, we will refer to this as the  $p, q$ -family.

## VI. COHERENCE AND SUB-POISSONIANITY

In this section, we employ Eqs. (30) and (31) to compute the quantities  $\mathfrak{C}$  and  $Q$ , respectively, for our three

families of laser models (33), (39) and (45). In doing so, we systematically explore the parameter space that is characteristic to each family to ascertain the influence that these parameters have on the coherence and Mandel- $Q$  parameter for each of the laser beams. We note that throughout this section, and for the remainder of this Paper, we let  $\mathcal{N} = 1$  to set a convenient unit for time.

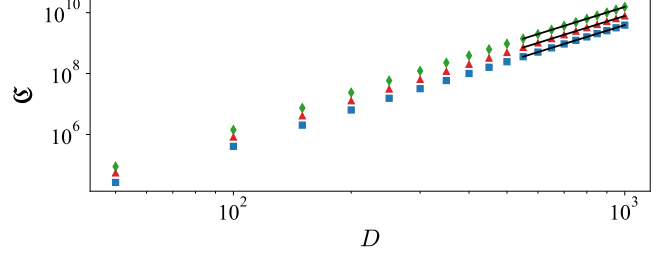


FIG. 4. iMPS calculations of the beam coherence for our three families of laser models as a function of dimension  $D = 2\mu + 1$ . Squares correspond to the laser family with the partially-isometric, Markovian gain model ( $p$ -family); triangles to the non-isometric, Markovian gain model ( $p, \lambda$ -family); and diamonds to the partially-isometric, non-Markovian gain model ( $p, q$ -family). Parameters are chosen such that beam coherence is maximized, these are  $p = 4.1479$ ,  $(p, \lambda) = (4.1479, 0.5)$  and  $(p, q) = (4.1479, -1.0)$  for each family, respectively. Solid black lines are fits to the data for  $D \in [550, 1000]$ , assuming a power law. Respectively, these are  $\mathfrak{C} = 0.0040D^4$ ,  $\mathfrak{C} = 0.0082D^4$  and  $\mathfrak{C} = 0.0140D^4$ .

As an initial result, we show that Heisenberg-limited scaling for the coherence may be realized in each of our three families of laser models. Fig. 4 shows iMPS calculations of  $\mathfrak{C}$  for each family plotted against the “cavity” dimension,  $D$ , ranging between  $D = 50$  and  $D = 1000$ . In this plot, the particular choice of the other parameters are  $p = 4.15$  for the  $p$ -family,  $p = 4.15$  and  $\lambda = 0.5$  for the  $p, \lambda$ -family, and  $p = 4.15$  and  $q = -1.0$  for the  $p, q$ -family. These parameter values are those which maximize  $\mathfrak{C}$  in each family. Fitting a power law  $\mathfrak{C} = c\mu^w$  (recalling that  $\mu = (D - 1)/2$ ) indicates that the coherence scales with the fourth power of  $\mu$  in each case. By construction, each of these families of laser models satisfy the first three conditions on the laser and its beam (that is, One Dimensional Beam, Endogenous Phase and Stationary Statistics) [1]. In Appendix B, we verify numerically that Eqs. (10a) and (10b) are satisfied, therefore demonstrating that Condition 4 is also fulfilled. From this, we may say that for these particular parameter values, these laser families all perform at the Heisenberg limit. Moreover, we find that the largest coherence is attained within the  $p, q$ -family, with the prefactor  $c$  in this optimized model being approximately four times larger than that for the  $p$ -family, and approximately twice as large as that for the  $p, \lambda$ -family.

Looking at influence of the characteristic parameters in more detail now, we first direct our focus towards the  $p$ -family, which is the most straightforward of the three.

Bringing one's attention to Fig. 5a, a number of qualitative statements can be made with regard to the behaviour of the coherence for this family from this plot. The red dots in Fig. 5a show iMPS calculations of the coherence normalized to its maximal value,  $\mathfrak{C}_0$ , as a function of the parameter  $p$  for a “cavity” of fixed dimension  $D = 1000$ . As  $p$  is increased from its lowest value, a rapid increase in the coherence is seen before reaching its maximum value at  $p \approx 4.1479$ . Increasing  $p$  above this optimal value, the coherence decreases monotonically from  $\mathfrak{C}_0$  at a relatively gradual rate. Strictly speaking, the location of the peak for the coherence has a small dependence on  $D$ , however from the analysis presented in Section VII we find that  $p = 4.1479$  maximizes the coherence in the asymptotic limit  $D \rightarrow \infty$ . Aside from this, the overall qualitative behaviour of the coherence seen in Fig. 5a was found to be independent of  $D$  for sufficiently large values of this parameter. Moreover, apart from a multiplicative factor, this behaviour with respect to  $p$  is preserved in the  $p, \lambda$ - and  $p, q$ -families regardless of  $\lambda$  and  $q$  (see Figs. 5c and 5e). Determining these multiplicative factors is the subject of the following section within this Paper, where analytical methods are employed to compute the coherence for each of these families of laser models.

This behaviour of the coherence with respect to  $p$  seen in Figs. 5a,c,e can be elucidated by considering what is shown in Figs. 5b,d,f. There, each data point (red dots) indicate, for a given value of  $p$ , the exponent  $w$  in the power law fitted to  $\mathfrak{C}$  when evaluated as a function of  $\mu$ . For instance, the plots in Fig. 4 show a particular example of this for  $p = 4.15$  and similar raw data is used to determine each data point shown in Figs. 5b,d,f for the various values of  $p$  considered. We again make the point to emphasize that these plots are independent of the parameters  $\lambda$  and  $q$ , and therefore the scaling of the coherence with  $\mu$  for each family depends only on  $p$ . In particular, we find that two distinct regimes may be identified for the behaviour of the coherence with respect to  $p$ . For values  $p \lesssim 3$ , the coherence appears to be sub-Heisenberg-limited, with the exponent roughly obeying the formula  $w = p + 1$ . This explains the rapid change in the coherence that is seen in Figs. 5a,c,e for these relatively low values of  $p$ . On the other hand, for values  $p \gtrsim 3$ ,  $w$  becomes constant and the coherence is Heisenberg-limited, being proportional to  $\mu^4$ . Although values  $p > 6$  are not shown here, it was found that this scaling is preserved for larger choices of  $p$ . This implies that the monotonic decrease in the coherence as a function of  $p$  above the optimal value of  $p \approx 4.1479$  seen in Figs. 5a,c,e is a result of the specific form of prefactor  $c$  in the power law  $\mathfrak{C} = c\mu^w$ , and not the exponent  $w$ . Heuristic arguments to explain the behaviour of  $w$  between these two distinct regimes are provided in Section VII.

It is more interesting, however, to view the behaviour of the coherence in conjunction with that of the  $Q$ -parameter of the output field shown in Fig 6. In Fig 6a

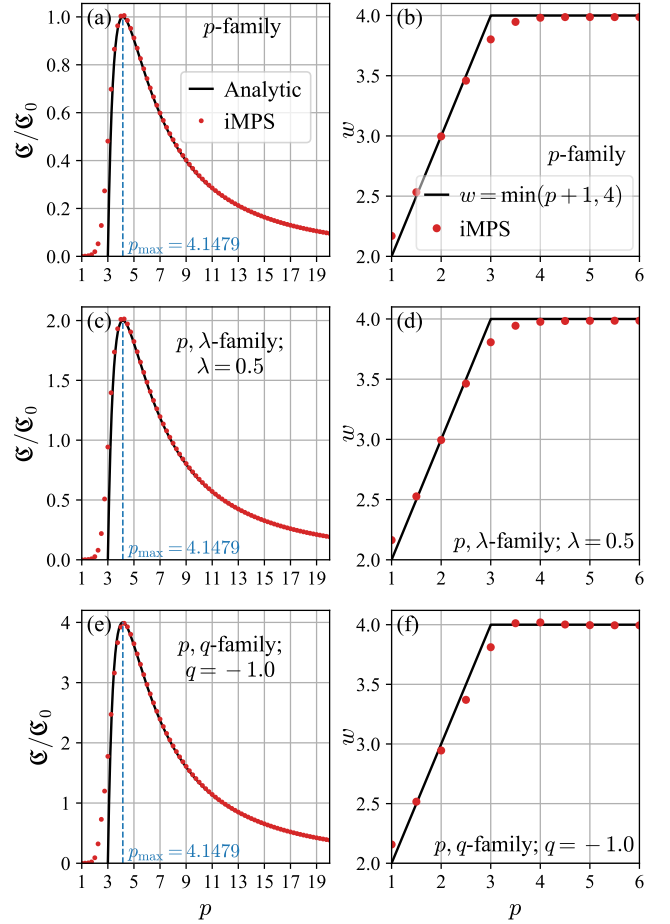


FIG. 5. (a,c,e): iMPS calculations of the beam coherence (red dots) for the  $p$ -,  $p, \lambda$ - and  $p, q$ -families of laser models described in the text as a function of  $p$  for a cavity dimension  $D = 1000$ . These values for the coherence have been normalized to the maximum value of that obtained from the  $p$ -family, for which  $p = 4.1479$ . Solid black curves show the corresponding formulae for each family of models given by Eqs. (52), (57a) and (57b). Additional choice of parameters for the sub-Poissonian laser families are  $\lambda = 0.5$  for the  $p, \lambda$ -family and  $q = -1.0$  for the  $p, q$ -family, which yield maximum photon noise reduction in the beam. (b,d,f): Exponent  $w$  (red dots) from the result of fitting  $\mathfrak{C} = c\mu^w$  for particular choices of  $p$ , obtained for iMPS calculations up to bond dimension  $D = 1000$  for the three families of laser models shown in the left-hand panels of this figure. Solid black lines depict  $w = \min(p + 1, 4)$  as a guide for the eye.

we provide a density plot of the coherence as a function of  $p$  and  $\lambda$  for the  $p, \lambda$ -family for  $D = 1000$ . Recall that for  $\lambda = 0.0$ , the  $p, \lambda$ -family reduces to the  $p$ -family. In this case, the system exhibits a flat gain such that  $\hat{G}^{(p, \lambda=0)}$  is essentially a finite version of the Susskind-Glogower operator [53]. Assuming a cavity state with negligible coefficient in its top level,  $|n = D - 1\rangle$ , the action of this operator will preserve the phase statistics. Therefore, essentially no phase noise will be added via the gain process in this scenario [54]. On the other hand, Fig 6a shows



that for a given value of  $p$ , the coherence is maximized by choosing  $\lambda = 0.5$ , for which  $\mathfrak{C}$  is twice that for the  $p$ -family with the same value of  $p$ . In this situation, a symmetry is imposed on the system where the matrix elements for the gain and loss operators are defined as reciprocals to one another. Given this observation, it is apparent that reducing the phase noise induced by the loss mechanism at the expense of that induced by the gain, to an extent, is advantageous to increase the coherence.

In Fig. 6b, we plot  $Q$  for the  $p, \lambda$ -family against the same parameters in Fig. 6a. This shows that the photon statistics are independent of  $p$ , and that the beam for the  $p$ -family is always characterized by Poissonian photon statistics ( $Q = 0.0$ ). We however find that  $Q$  is minimized to a value of  $-0.5$  when  $\lambda = 0.5$ , which corresponds to a 50% reduction in the number fluctuations of the laser beam below the shot noise limit for long counting intervals. This minimum value of  $Q$  is found at exactly the same values which maximize the coherence within this family of laser models. Given this apparent “win-win” situation between  $\mathfrak{C}$  and  $Q$  for the  $p, \lambda$ -family leads us to the conclusion that *there is no trade-off between coherence and sub-Poissonianity for Heisenberg-limited lasers*.

As we have pointed out earlier, this minimum of  $Q = -0.5$  seen for the  $p, \lambda$ -family can be surpassed and complete noise reduction for long times ( $Q = -1.0$ ) is achievable by employing a regular pumping mechanism within the laser. This is exactly what we demonstrate in Fig. 6d, which displays the  $Q$  parameter for our  $p, q$ -family against the parameters  $p$  and  $q$ , again with  $D = 1000$ . As anticipated, we find that the  $Q$  parameter of the output field mirrors exactly that of  $q$ , the Mandel- $Q$  parameter of the pumping mechanism. For completely regular pumping,  $q \rightarrow -1$ , we find  $Q \rightarrow -1$  (regardless of  $p$ ), corresponding to 100% reduction in the photon number fluctuations in the beam for long counting times. In addition to this, for a given  $p$ , we find that  $\mathfrak{C}$  is maximized with  $q \rightarrow -1$ , which is approximately four times that for the  $p$ -family for the same value of  $p$  (see Fig. 6c). This takes the results for the  $p, \lambda$ -family a step further, by demonstrating that this synergistic effect between coherence and sub-Poissonianity in the output field persists in Heisenberg-limited lasers, even when extreme measures are taken to completely eliminate the photon noise in the beam. These results together mark a generalisation of the findings from previous studies relating to lasers with linear-loss [21, 44, 49, 50], where we have extended the notion that a trade-off between  $\mathfrak{C}$  and  $Q$  does not necessarily exist, even for lasers with a phase diffusion rate that is far smaller than any laser model previously studied. Moreover, these results show that there is a “win-win” relationship between these two quantities, as minimizing  $Q$  comes hand-in-hand with a maximization of  $\mathfrak{C}$ .

It is difficult to pinpoint the reason for this synergistic relationship between beam coherence and sub-Poissonianity in general. Indeed, within the  $p, \lambda$ -family,

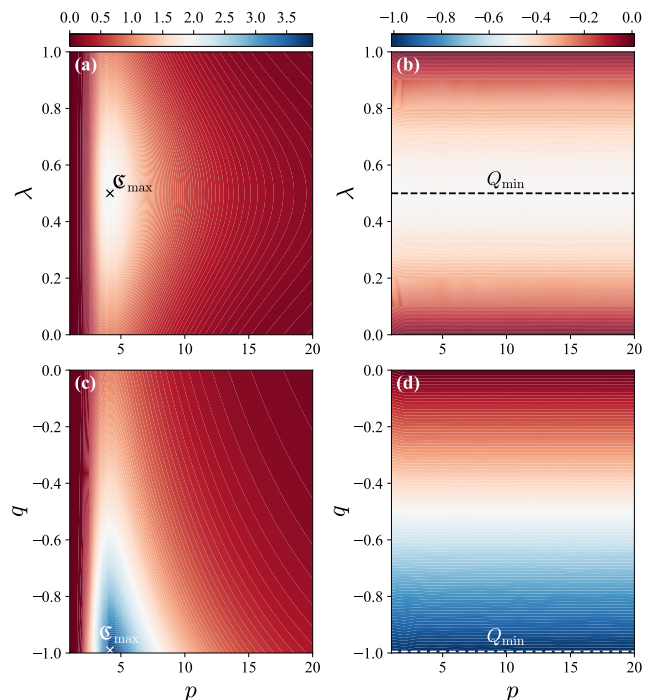


FIG. 6. (a,c): iMPS calculations of beam coherence for the  $p, \lambda$ -family and  $p, q$ -family, respectively, and with cavity dimension  $D = 1000$ . These values of the coherence have been normalized to the maximum of that obtained for the  $p$ -family of lasers for  $D = 1000$ . Crosses show the parameter choices which yield maximum coherence, according to Eqs. (57a) and (57b), which are located at  $(p, \lambda) = (4.1479, 0.5)$  and  $(p, q) = (4.1479, -1.0)$ , respectively. (b,d): Same as that shown for (a,c), but with normalized coherence substituted with the Mandel- $Q$  parameter of the beam. Dashed lines show the parameter choices which yield minimum  $Q$  values, being  $Q = -0.5$  and  $Q = -1.0$  for the  $p, \lambda$ -family and  $p, q$ -family, respectively.

the exact mechanism behind this remains unclear. However, for the  $p, q$ -family there is a fairly straightforward interpretation for this behaviour. That is, when the regularity of the pump is increased by reducing the value of  $q$ , the matrix elements of the loss operator,  $L_n^{(p, -q/2)}$ , defined in Eq. (34b) become “flatter” as a function of  $n$  in order to preserve the steady state cavity distribution for a given value of  $p$ . As a consequence of this, the cavity state is exposed to a loss operation which will add less phase noise to the system (recalling also that the gain, being quasi-isometric, will add a negligible amount of phase noise to the beam). This will lead to an increase in the coherence of the beam, compared to a more random pumping scenario for higher values of  $q$ .

Another observation to make here is with regard to the correlation time of the photon statistics. For the sub-Poissonian laser models we consider, the correlation time of  $g_{ps}^{(2)}(\tau)$  is much shorter than the coherence time, such that a significant degree of sub-Poissonianity in the beam may be observed for counting intervals where the

phase of the beam remains fairly well-defined. This can be seen by considering both the  $p$ ,  $\lambda$ - and  $p$ ,  $q$ -families under the choice of parameters which minimize  $Q$ ; respectively, these are  $\lambda \rightarrow 0.5$  and  $q \rightarrow -1$  (regardless of the value of  $p$ ). It is shown in Appendix B, in both scenarios, that  $1 - g_{\text{ps}}^{(2)}(0) = \Theta(\mathfrak{C}^{-1/2})$ . Assuming an exponential decay for these functions (this is not strictly true for relatively small values of  $p$ , but is reasonable to assume for this qualitative argument), obtaining values of  $Q = \Theta(1)$  with these parameter choices, as was demonstrated above, requires the correlation time to be  $\Theta(\mathfrak{C}^{1/2})$  in accordance with Eq. (9). Interestingly, this is of the same order as optimal time for the filtering/retrofiltering measurements used in Theorem 1 (recalling the choice  $\mathcal{N} = 1$ ), which is a factor of  $\mu^{-2}$  shorter than the coherence time of these laser models. This detail regarding the photon statistics of these laser families will be explored in more depth in future work.

## VII. GENERALIZED FORMULAE FOR LASER COHERENCE

In this final section of results, we derive formulae for the laser coherence of our three families of laser models for a large range of values for  $p$ . These formulae are shown to be valid in the asymptotic limit  $D \rightarrow \infty$  for values  $p \gtrsim 3$ , for which Heisenberg-limited scaling,  $\mathfrak{C} \sim \mu^4$ , is achieved as indicated in Figs. 5b,d,f. In addition to this, although expressions for  $\mathfrak{C}$  that are valid for  $p \lesssim 3$  are unable to be obtained here, this analysis does give insight to the change in the exponent for the power law  $\mathfrak{C} = c\mu^w$  to sub-Heisenberg-limited scaling for these parameter values.

### A. $p$ -family

We begin by focusing on the  $p$ -family, which exhibits Poissonian beam photon statistics. In order to derive an expression for the laser coherence, we appeal to the fact that the first-order Glauber coherence function is well-approximated by that of an ‘ideal’ laser state given by Eq. (6), that is,

$$g^{(1)}(t) \approx \exp(-\ell|t|/2). \quad (46)$$

Moreover, we assume that this holds to a first order approximation for an arbitrarily short time interval  $\delta t$ , which allows one to write

$$\text{Tr} \left[ \hat{L}^{(p,0)\dagger} \mathcal{L}_{\text{M}}^{(p,0)} \left( \hat{L}^{(p,0)} \rho_{ss} \right) \right] \approx -\frac{\ell}{2}. \quad (47)$$

This is justified on inspection of Fig. 7a, which shows numerical calculations of  $g^{(1)}(t)$  overlapped with the function  $e^{-\ell|t|/2}$ , with the linewidth also computed numerically. For short times, we see that the approximation of Eq. (47) is reasonable.

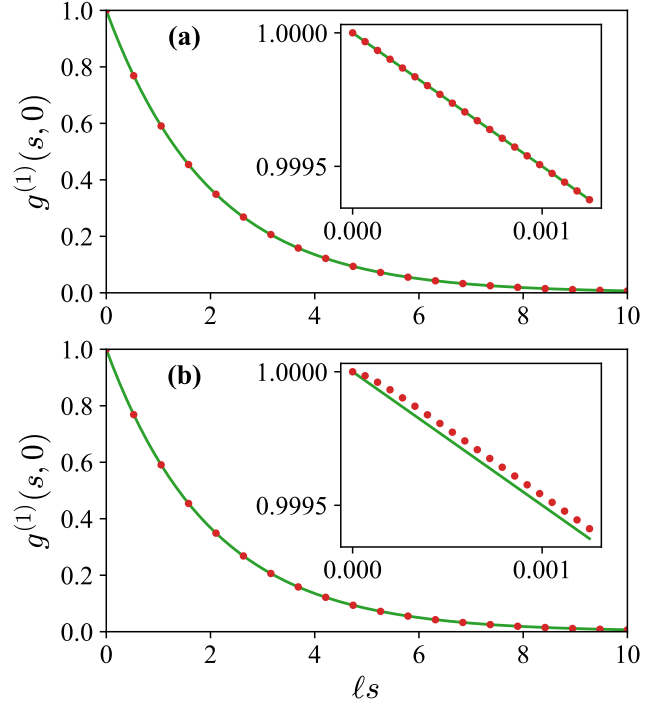


FIG. 7. (a): iMPS calculations (red dots) of the first-order Glauber coherence function  $g^{(1)}(s, 0)$  for the  $p$ -family of laser models, with  $p = 4.15$  and  $D = 300$  over 10 coherence times,  $1/\ell$ . Green lines show the first-order Glauber coherence function for an ideal laser state,  $g^{(1)}(s, 0) = \exp(-\ell|s|/2)$ . The inset give the same as what is shown in the larger panel, yet over a much shorter time scale such that  $\exp(-\ell|s|/2) \approx -\ell|s|/2$ . (b): Same as that shown in (a), but for the the  $p$ ,  $\lambda$ -family of laser models where  $\lambda = 0.5$ . We have omitted showing this for the  $p$ ,  $q$ -family of laser models as these results are essentially the same as those shown for the  $p$ ,  $\lambda$ -family in panel (b), where deviations occur between the laser model's and ideal laser's  $g^{(1)}(s, 0)$  behaviour for very short times when sub-Poissonian photon statistics are imposed on the beam.

Using the photon-number basis  $\{|n\rangle\}$  to evaluate the trace in Eq. (47), we can write it as the sum

$$\sum_{n=0}^{D-1} f_n^{(p,0)} \equiv \text{Tr}[\hat{L}^{(p,0)\dagger} \mathcal{L}_{\text{M}}^{(p,0)} (\hat{L}^{(p,0)} \rho_{ss})]. \quad (48)$$

The elements  $f_n^{(p,0)}$  may be written in terms of the elements of the steady-state cavity distribution,

$$f_n^{(p,0)} = \begin{cases} 0 & n = 0, \\ \frac{-\rho_0^2}{2\rho_1} & n = 1, \\ \frac{\rho_{D-2}}{2} \left( \sqrt{\frac{\rho_{D-3}}{\rho_{D-2}}} - \sqrt{\frac{\rho_{D-2}}{\rho_{D-1}}} \right)^2 - \frac{\rho_{D-2}}{2} & n = D-1, \\ \frac{-\rho_{n-1}}{2} \left( \sqrt{\frac{\rho_{n-2}}{\rho_{n-1}}} - \sqrt{\frac{\rho_{n-1}}{\rho_n}} \right)^2 & \text{otherwise.} \end{cases} \quad (49)$$

If one can evaluate the sum given by Eq. (48), then an estimate for the linewidth of the laser can be obtained.

This does not appear trivial at first glance. Luckily, significant simplifications can be made by investigating the behaviour of  $f_n^{(p,0)}$  against the parameter  $p$ , which is depicted in Figs. 8a and 8b for two different choices of cavity dimension. The solid black lines in these plots show the exact elements of the sum for values of  $p = 3, 4, 5$ . From this, along with Eq. (49), we can identify two distinct regimes based on the dominant terms in the sum and how they change with  $p$  for  $D \gg 1$ . In particular, terms near the midpoint ( $n \approx \mu$ ) are of order  $O(D^{-5})$  and, roughly speaking, there are  $O(D)$  elements that scale in this manner. Therefore, it would be expected that together these terms would contribute a quantity of order  $O(D^{-4})$  to the total sum. On the other hand, we find that the edge elements have a greater dependence on the parameter  $p$ , where in the extreme cases (e.g.,  $n = 1$  and  $n = D - 1$ ) they are of order  $O(D^{-(p+1)})$ —note the sudden “flip” in the plots in moving from  $p > 4$  to  $p < 4$  as these edge elements suddenly become the largest terms in  $f_n^{(p,0)}$ . The first of these regimes is therefore identified for values  $p > 3$ , where the sum is dominated by the elements around the midpoint, while the second is identified for values  $p < 3$ , where the edge elements are instead dominant. As the coherence is directly proportional to the inverse of  $\sum_n f_n^{(p,0)}$  (assuming that Eq. (47) holds), from this behaviour one should expect a change in the scaling of  $\mathfrak{C}$  with  $\mu$  when moving between these regimes. This competition between the central and edge elements of  $f_n^{(p,0)}$  therefore explains the behaviour observed in Fig. 5b, as the exponent changes from  $w \approx p + 1$  for  $p < 3$ , to  $w \approx 4$  for  $p > 3$ .

Guided by this insight, we now attempt to evaluate Eq. (48) for  $p > 3$  by performing a Taylor series expansion of  $f_n^{(p,0)}$  about the midpoint  $n = \mu$ , which, to leading order in  $1/(D + 1)$ , is

$$f_n^{(p,0)} \approx -\frac{\pi^{9/2} p^2}{8(D+1)^5} \frac{\Gamma\left(\frac{2+p}{2}\right)}{\Gamma\left(\frac{1+p}{2}\right)} \cdot \left(1 + \cot^2\left(\pi \frac{n+1}{D+1}\right)\right)^2 \sin^p\left(\pi \frac{n+1}{D+1}\right). \quad (50)$$

The validity of this approximation can be visualised in Figs. 8a and 8b, where the marked points correspond to an evenly-spaced subset of the elements within the approximation of Eq. (50). These are plotted on top of the exact elements of the sum given by the solid lines. Even for moderately large values of  $D$ , this approximation is very accurate for  $p > 3$ .

It is possible to evaluate the sum within this approximation by taking the limit  $D \rightarrow \infty$  and converting it to an integral by defining the continuous parameter

$x := \pi(n + 1)/(D + 1)$ , which takes values in  $[0, \pi)$ :

$$\lim_{D \rightarrow \infty} \sum_{n=0}^{D-1} f_n^{(p,0)} = -\frac{\pi^{7/2} p^2}{8D^4} \frac{\Gamma\left(\frac{2+p}{2}\right)}{\Gamma\left(\frac{1+p}{2}\right)} \cdot \int_0^\pi dx (1 + \cot^2(x))^2 \sin^p(x). \quad (51)$$

After evaluating the integral in the RHS of this equation, a formula for the linewidth is obtained from Eq. (47) and, in turn, the coherence for the  $p$ -family,

$$\mathfrak{C}^{(p,0)} = \frac{256}{\pi^4 p^2} \frac{\Gamma\left(\frac{p+1}{2}\right) \Gamma\left(\frac{p-2}{2}\right)}{\Gamma\left(\frac{p+2}{2}\right) \Gamma\left(\frac{p-3}{2}\right)} \mu^4, \quad (D \rightarrow \infty, p > 3). \quad (52)$$

Eq. (52) is compared with the numerical evaluation of  $\mathfrak{C}$  for  $D = 1000$  in Fig. 5a. Excellent quantitative agreement is observed between these two methods of analysis for all values of  $p \gtrsim 3$ . Indeed, Eq. (52) correctly predicts the peak in the coefficient for the power law  $\mathfrak{C} = c\mu^4$ , being at  $p = 4.1479$ . This optimal value can be found by evaluating the stationary point for the prefactor in the above equation as a function of  $p$ . We begin to see significant deviations between our numerical and analytical results within the lower extreme for which Eq. (52) is defined, where  $3 < p < 4$ . We expect that numerical results for larger system sizes would yield better agreement with the analytical formula in this region, although showing this is exceedingly computationally expensive and therefore not addressed in the present Paper.

## B. Sub-Poissonian Laser Families

Unfortunately, one cannot directly apply the arguments detailed above to obtain formulae for the coherence of the more general  $p, \lambda$ - and  $p, q$ -families, which exhibit sub-Poissonian beam photon statistics. The reason for this can be seen in Fig. 7b, which shows  $g^{(1)}(\tau)$  for these two families for the choice of parameters that maximize  $\mathfrak{C}$  and minimize  $Q$ , along with that produced by an ideal beam,  $g^{(1)}(\tau) = \exp(-\ell|\tau|/2)$ . Here, we can see that although the first order Glauber coherence functions of these families are essentially identical to the characteristic exponential decay exhibited by an ideal laser for relatively long times, small deviations between these two functions are observed for relatively short correlation times. This invalidates the first-order approximation given in Eq. (47).

In order to work around this, we take a heuristic approach and find that replacing Eq. (47) with the ansatz

$$\sum_{n=0}^{D-1} (\mathcal{L} \varrho_c^{\phi=0})_{n,n+1} \approx -\frac{\ell}{2}, \quad (53)$$

corrects the small deviation seen in the short-time behaviour observed in Fig. 7b. Here we utilize the state  $\varrho_c^\phi$ ,

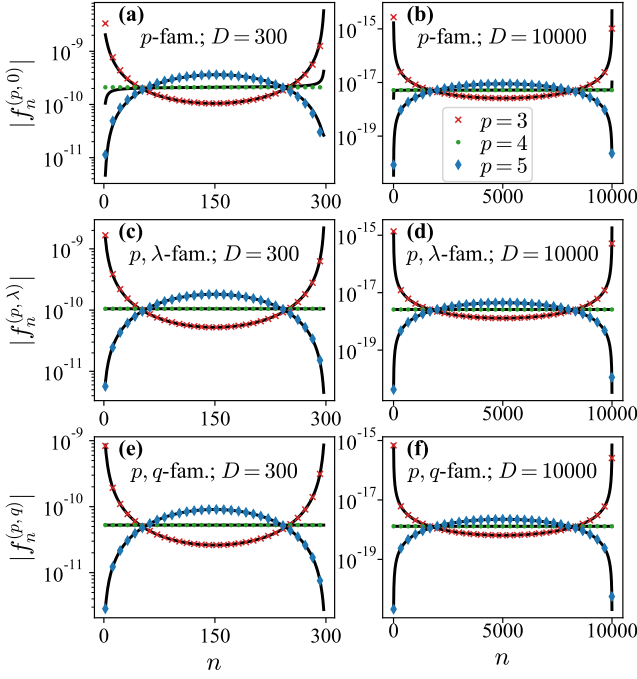


FIG. 8. (a): Absolute values of the diagonal elements defined by  $f_n^{(p,0)} = [\hat{L}^{(p,0)\dagger} \mathcal{L}_M^{(p,0)} (\hat{L}^{(p,0)} \rho_{ss})]_{n,n}$  for cavity dimension  $D = 300$ . Solid black lines show the exact elements, while markers indicate the elements obtained from the approximation given in Eq. (50). Respectively, red crosses, green dots and blue diamonds correspond to the cases of  $p = 3, 4, 5$ , respectively. Note that only a subset of equally spaced elements are marked here for clarity. (b): Same as for (a), but with an increased cavity dimension to  $D = 10000$ . (c-d): Same as (a-b), respectively, but for the sum defined by  $f_n^{(p,\lambda)} = (\mathcal{L}_M^{(p,\lambda)} \varrho_c^{\phi=0})_{n,n+1}$  and with  $\lambda = 0.5$ . (e-f): Same as (a-b), respectively, but for the sum defined by  $f_n^{(p,q)} = (\mathcal{L}_{NM}^{(p,q)} \varrho_c^{\phi=0})_{n,n+1}$  and with  $q = -1$ .

which is a projector onto the pure cavity state

$$|\psi^\phi\rangle_c = \sum_{n=0}^{D-1} \sqrt{\rho_n} e^{i\phi n} |n\rangle, \quad (54)$$

such that the uniformly weighted ensemble reproduces the incoherent steady-state of our families of laser models, i.e.,  $\int_0^{2\pi} \varrho_c^\phi d\phi / (2\pi) = \sum_{n=0}^{D-1} \rho_n |n\rangle \langle n|$ . The LHS of Eq. (53) can be thought as an average of the decay of the off-diagonal components of this pure cavity state, however we do not provide a rigorous justification for this equation. Regardless, it will be shown that this expression provides a remarkably powerful method of computing the coherence. In particular, by starting with this instead of Eq. (47) and following the steps which led to the general expression of the laser coherence for the  $p$ -family, similar expressions are able to be derived for the  $p, \lambda$ - and  $p, q$ -families, which are just as accurate.

With this caveat, we proceed to derive a general formula for the coherence of our  $p, \lambda$ - and  $p, q$ -families

of laser models. Mirroring the steps outlined in Part A of this section, we have the sum elements  $f_n^{(p,\lambda)} = (\mathcal{L}_M^{(p,\lambda)} \varrho_c^{\phi=0})_{n,n+1}$  and  $f_n^{(p,q)} = (\mathcal{L}_{NM}^{(p,q)} \varrho_c^{\phi=0})_{n,n+1}$ , which can be expressed as

$$f_n^{(p,\lambda)} = \frac{-\sqrt{\rho_n \rho_{n+1}}}{2} \left\{ \left[ \left( \frac{\rho_{n-1}}{\rho_n} \right)^{\frac{(1-\lambda)}{2}} - \left( \frac{\rho_n}{\rho_{n+1}} \right)^{\frac{(1-\lambda)}{2}} \right]^2 + \left[ \left( \frac{\rho_{n+1}}{\rho_n} \right)^{\frac{\lambda}{2}} - \left( \frac{\rho_{n+2}}{\rho_{n+1}} \right)^{\frac{\lambda}{2}} \right]^2 \right\}, \quad (55a)$$

$$f_n^{(p,q)} = \frac{-\sqrt{\rho_n \rho_{n+1}}}{2} \left[ \left( \frac{\rho_{n-1}}{\rho_n} \right)^{\frac{(2+q)}{4}} - \left( \frac{\rho_n}{\rho_{n+1}} \right)^{\frac{(2+q)}{4}} \right]^2. \quad (55b)$$

Performing a Taylor series expansion about the midpoint of  $n = \mu$  gives

$$f_n^{(p,\lambda)} \approx (2\lambda^2 - 2\lambda + 1) f_n^{(p,0)}, \quad (56a)$$

$$f_n^{(p,q)} \approx (1 + q/2)^2 f_n^{(p,0)}. \quad (56b)$$

Eqs. (55) are compared with Eqs. (56) in Fig. 8c-f. It can be seen there that the behaviour of the edge elements for these sums with respect to  $p$  is the same as that for the  $p$ -family, and the approximations given in Eq. (56) are very accurate. Applying the same arguments as those used to move from Eq. (50) to Eq. (52) leads directly to an expression of the coherence for the  $p, \lambda$ - and  $p, q$ -families, respectively, with

$$\mathfrak{C}^{(p,\lambda)} = \frac{\mathfrak{C}^{(p,0)}}{2(\lambda - 1/2)^2 + 1/2}, \quad (D \rightarrow \infty, p > 3), \quad (57a)$$

$$\mathfrak{C}^{(p,q)} = \frac{\mathfrak{C}^{(p,0)}}{(1 + q/2)^2}, \quad (D \rightarrow \infty, p > 3). \quad (57b)$$

Eqs. (57a) and (57b) correctly predict the coherence for the respective families of laser models for the same values of  $p$  for which Eq. (52) is valid. This agreement is also shown in Figs. 5c and 5e, where the two equations given directly above are compared with iMPS calculations of the coherence for  $D = 1000$  for specific parameter choices that minimize the  $Q$  parameter of the beam.

## VIII. CONCLUSION

In this Paper, we have expanded upon the seminal result of Ref. [1] by providing a study of lasers which exhibit Heisenberg-limited coherence as well as sub-Poissonian



beam photon statistics. Much of this serves to supplement the companion Letter [2], which summarizes the key results of this study, while also providing many additional findings that develop our understanding of laser models exhibiting Heisenberg-limited coherence.

In particular, we have detailed the generalized proof of the upper bound for laser coherence, showing that  $\mathfrak{C} = O(\mu^4)$  is the Heisenberg limit for a much broader class of lasers. This class of lasers encompass certain beams which can have a Mandel- $Q$  parameter for long photon counting durations on the beam arbitrarily close to the minimum of  $Q = -1$  [31]. From this result, we introduced three new families of laser models; all of which were shown to demonstrate Heisenberg scaling of  $\mathfrak{C}$  with  $\mu$  under appropriate parameter choices. Two of these families, namely the  $p, \lambda$ -family and  $p, q$ -family, which respectively exhibited a non-isometric, Markovian gain process (parameterized by  $\lambda$ ) and a partially-isometric, non-Markovian gain process (parameterized by  $q$ ), were shown to have sub-Poissonian beam photon statistics, with negative values of  $Q$  under particular parameter values. For the  $p, \lambda$ -family, a minimum of  $Q = -0.5$  was obtained, corresponding to a 50% reduction of the photon noise in the beam below the shot-noise limit at cavity resonance. This was obtained for the choice of parameter  $\lambda = 0.5$ , corresponding to a scenario where the matrix elements specifying gain and loss into and out of the laser cavity were defined as reciprocals to one another. For the  $p, q$ -family, complete photon noise reduction in the beam was acquired ( $Q = -1$ ) when the pumping of excitations into the cavity was done so in a completely regular manner, corresponding to the choice of parameter  $q \rightarrow -1$ .

This in turn led to the central result of this Paper, and that of the companion Letter to this work [2], as it was found that the exact choice of parameters which minimize the  $Q$  parameter of the beam (i.e., those which maximize the degree of sub-Poissonianity) within the two sub-Poissonian families of laser models also maximized the coherence. In particular, in the asymptotic limit  $\mu \rightarrow \infty$ , it was found that  $\lambda$  influences the coherence of the  $p, \lambda$ -family by modulating that of the  $p$ -family with a Lorentzian function centered at  $\lambda = 0.5$ , with a peak of 2, and a FWHM of  $\Delta\lambda = 1$  (see Eq. 57a)). Furthermore,  $q$  was found to influence the coherence of the  $p, q$ -family by modulating that of the  $p$ -family with the function  $1/(1 + q/2)^2$  (see Eq. (57b)). This led to the conclusion that a trade-off between coherence and sub-Poissonianity in Heisenberg-limited laser models does not exist. To the contrary, taking measures to minimize  $Q$  also gives rise an increase in  $\mathfrak{C}$  for the specific laser models studied here. This trade-off is well-known to not exist in laser models with coherence at the SQL [21]. The result at hand therefore marks a generalization of these results to laser models which have a vastly smaller (Heisenberg-limited) rate of phase diffusion.

Along with this result, we were also able to derive formulae for the coherence of the three families of laser mod-

els which accurately reproduced the numerical results for large  $\mu$ . These formulae hold in the regime defined by  $p \gtrsim 3$ , where the laser families exhibit Heisenberg-limited coherence,  $\mathfrak{C} = \Theta(\mu^4)$ , in the asymptotic limit  $\mu \rightarrow \infty$ . In particular, these formulae suggested that  $p = 4.1479$  is optimal to maximize the coherence in each family, which deviates slightly from the value  $p = 4$  used as an ansatz in Ref. [1]. Although these formulae do not readily generalize to the regime of  $p \lesssim 3$ , where the  $\mu^4$  scaling of the coherence is lost, we were able to provide heuristic arguments based on our analysis to explain this change of scaling.

Looking outwards towards future work, a number of avenues are open. Firstly, as we have not provided any rigorous justification for the use of Eq. (53), one could investigate why this ansatz serves as such an accurate formula to predict the linewidth. In particular, why does this equation work in general for the  $p, \lambda$ - and  $p, q$ -families (i.e., those which exhibit sub-Poissonian beam statistics), while a simple first order expansion in  $t$  of Eq. (46) does not? Secondly, one could also explore the fundamental limits for laser coherence under different assumptions on the beam. For example, we believe the limit found in Ref. [1] can be tightened for a beam that is exactly describable by a coherent state undergoing pure phase diffusion. This would be a much stricter requirement on the beam compared to Condition 4 of both this Paper and that in Ref. [1], as it would also place constraints on the Glauber coherence functions given in Eq. (4) above second order. Preliminary numerical results suggest that this regime, where the beam may be described by a coherent state with diffusing phase, may be realised with our  $p$ -family in the limit  $D \rightarrow \infty$  and  $p \gg 1$ . These results will be presented in a future Paper.

## IX. ACKNOWLEDGEMENTS

The authors acknowledge the support of the Griffith University eResearch Service and Specialised Platforms Team and the use of the High Performance Computing Cluster ‘‘Gowonda’’ to complete this research. This work was supported by ARC Discovery Projects DP220101602 and an Australian Government RTP Scholarship.

### Appendix A: Mathematical Details for the $p, q$ -family; Steady-State and Approximate master equation

In this appendix we provide mathematical details relating to the family exhibiting the regularly pumped (non-Markovian), quasi-isometric gain model (i.e., the  $p, q$ -family) described by Eq. (45) in the main text. In particular, we demonstrate that in the asymptotic limit,  $D \rightarrow \infty$ , the cavity distribution at steady-state,  $\rho_n = \langle n | \rho_{ss} | n \rangle$ , for this family of models is characterised

by the elements

$$\rho_n = \alpha \sin^p \left( \pi \frac{n+1}{D+1} \right). \quad (\text{A1})$$

That is, it is the same as that for the other two families of laser models considered within this Paper. Additionally, we justify the various assumptions made throughout the derivation leading to the Master Equation (45) describing this family.

Addressing the cavity distribution first, the goal is to show that  $\lim_{D \rightarrow \infty} \mathcal{L}_{\text{NM}}^{(p,q)} \rho_{ss} = 0$ . From Eq. (45), we have (excluding edge elements, as they are of order  $O(D^{-(p+1)})$  and therefore negligible)

$$\begin{aligned} \langle n | \mathcal{L}_{\text{NM}}^{(p,q)} \rho_{ss} | n \rangle = & \left\{ (1-q) \frac{\rho_{n-1}}{\rho_n} + (q/2 - 1) \right. \\ & + (q/2) \frac{\rho_{n-2}}{\rho_n} + \left( L_{n+1}^{(p,-q/2)} \right)^2 \frac{\rho_{n+1}}{\rho_n} \\ & \left. - \left( L_n^{(p,-q/2)} \right)^2 \right\} \rho_n. \end{aligned} \quad (\text{A2})$$

On substituting the expression for  $L_n^{(p,-q/2)}$  given by Eq. (34b) in the main text with  $x \rightarrow -q/2 \in (-\infty, 1/2)$ , we have

$$\begin{aligned} \langle n | \mathcal{L}_{\text{NM}}^{(p,q)} \rho_{ss} | n \rangle = & \left\{ (1-q) \frac{\rho_{n-1}}{\rho_n} + (q/2 - 1) \right. \\ & + (q/2) \frac{\rho_{n-2}}{\rho_n} + \left( \frac{\rho_n}{\rho_{n+1}} \right)^{q/2} \\ & \left. - \left( \frac{\rho_{n-1}}{\rho_n} \right)^{(1+q/2)} \right\} \rho_n. \end{aligned} \quad (\text{A3})$$

It is possible to show using the elementary identity  $\sin(A \pm B) = \sin(A) \cos(B) \pm \cos(A) \sin(B)$  that

$$\frac{\rho_{n-1}}{\rho_n} = \left[ \cos \left( \frac{\pi}{D+1} \right) - \sin \left( \frac{\pi}{D+1} \right) \cot \left( \pi \frac{n+1}{D+1} \right) \right]^p. \quad (\text{A4})$$

For sufficiently large  $p$ , the distribution  $\rho_n$  is well-localized around its midpoint,  $\mu$ . In this scenario, the only relevant terms in Eq. (A3) will be those for which Eq. (A4) may be treated as a linear function of  $n$ , that is

$$\frac{\rho_{n-1}}{\rho_n} = 1 + \frac{p\pi^2}{(D+1)^2} (n+1-\mu) + O((D+1)^{-3}), \quad (\text{A5})$$

where  $n - \mu = O(1)$ . Substituting this expression into (A3), it is straightforward to show that all terms within the curly braces of lower order than  $O((D+1)^{-3})$  vanish. Therefore, Eq. (A1) rapidly converges to the actual steady-state distribution in the limit  $D \rightarrow \infty$  and  $1 \ll p \ll D$ .

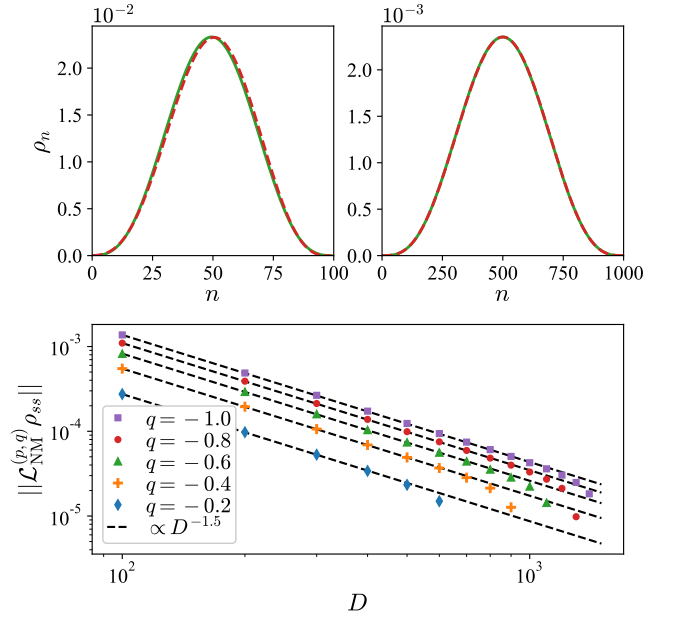


FIG. 9. Top panels: Exact steady-state cavity distribution computed numerically from Eq. (45) (red dashed lines) compared with the distribution defined by Eq. (A1) (solid green lines). Here, the choice of parameters are  $p = 3$  and  $q = -1.0$ . The top-left panel is for a relatively small cavity dimension ( $D = 100$ ), while the top-right panel is for  $D = 1000$ . Bottom panel: Frobenius norms, defined as  $\|\hat{A}\| = (\text{Tr}\{\hat{A}^\dagger \hat{A}\})^{-1/2}$ , of the matrix  $\mathcal{L}_{\text{NM}}^{(p,q)} \rho_{ss}$  plotted against cavity dimension,  $D$ , for  $p = 3$  and a range of values of  $q$ . Dashed black lines correspond to a power law with an exponent of  $-1.5$  as a guide for the eye.

To illustrate this point, we compare the distribution defined by Eq. (A1) to the exact steady-state of Eq. (45) computed numerically in the top panels of Fig. 9. Here, we have chosen  $q = -1$  and  $p = 3$ . Such a value of  $p$  is the smallest that we consider for our calculations of the coherence in Section VII and is much smaller than what would be required for the linearized treatment of the loss operators given in Eq. (A5). Regardless of this, we still find Eq. (A1) to be an excellent approximation of the actual steady-state distribution for the  $p, q$ -family. Even for moderately large values for the cavity dimension, such as that given in the right-hand top panel of Fig. 9 where  $D = 1000$ , we find the two distributions to be virtually indistinguishable.

In order to be more rigorous and demonstrate the validity of Eq. (A1) for more general values of  $p$ , we revert to numerical methods. In the bottom panel of Fig. 9, we show the Frobenius norms of  $\mathcal{L}_{\text{NM}}^{(p,q)} \rho_{ss}$  against cavity dimension,  $D$ , for  $p = 3$  (again, which is the smallest value of  $p$  for which our formula for the coherence, given by Eq. (57b), holds) and a range of values for  $q$ . Here, it is clear that for all values of  $q$ , this quantity converges to zero in the limit  $D \rightarrow \infty$ , as each of the matrix norms are  $o(D^{-1.5})$ .

Next, we justify the various approximations made in the steps of the derivation which led to Eq. (45), the master equation for the  $p, q$ -family of laser models. In that derivation, it was assumed that over some short time interval,  $\Delta t$ , the superoperators giving rise to the gain and loss of excitations within the cavity (see Eqs. (41) in the main text) act independently. For this to be the case, the action of the superoperators  $\mathcal{D}[\hat{L}^{(p, -q/2)}]$  and  $(\mathcal{G} - 1) = \mathcal{D}[\hat{G}^{(p, 0)}] + \mathcal{D}[\hat{\Pi}_{\text{top}}]$  on the cavity state need to be small, in some sense. To demonstrate this, we consider their action on the pure cavity state

$$\varrho_c^\phi = \sum_{n,m=0}^{D-1} \sqrt{\rho_n \rho_m} e^{i\phi(n-m)} |n\rangle \langle m|. \quad (\text{A6})$$

This state was also briefly introduced in Section VII of the main text to derive formulae for the coherence of our families of laser models; it is defined in such a way that a uniformly weighted mixture reproduces the cavity steady-state,  $\int_0^{2\pi} \varrho_c^\phi d\phi / (2\pi) = \sum_{n=0}^{D-1} \rho_n |n\rangle \langle n|$ . To motivate this choice of state, we assume that throughout the evolution of the system, the cavity state can be expressed as a mixture of states within the ensemble  $\{\varrho_c^\phi, d\phi / (2\pi)\}$ ; or in other words, we assume that this ensemble is physically realizable [55]. A rigorous investigation of the validity of this pure state assumption will be addressed in a future Paper.

In Fig. 10 we show the Frobenius norms of the matrices  $\mathcal{D}[\hat{L}^{(p, -q/2)}]_{\varrho_c^{\phi=0}}$  and  $(\mathcal{G} - 1)_{\varrho_c^{\phi=0}}$  against cavity dimension,  $D$ , with  $q = -1$  and  $p = 3$ . Fitting a power law to these points indicate that these Frobenius norms are  $O(D^{-1})$ . This implies that over the time interval,  $\Delta t$ , one may treat the gain and loss processes independently if one takes  $\mathcal{N}\Delta t \ll D$ , in which case

$$\rho(t + \Delta t) \approx (1 + (\mathcal{G} - 1))^{n(\Delta t)} \rho(t) + \mathcal{N}\Delta t \mathcal{D}[\hat{L}^{(p, -q/2)}] \rho(t). \quad (\text{A7})$$

Recall that we let  $n(\Delta t) = \mathcal{N}\Delta t + \sqrt{\mathcal{N}(q+1)}\Delta W$  represent the number of excitations gained by the cavity in the interval  $\Delta t$ . Additionally, since we have  $(\mathcal{G} - 1)_{\varrho_c^{\phi=0}} = O(D^{-1})$ , a binomial expansion to second order in  $(\mathcal{G} - 1)$  is reasonable, therefore validating Eq. (44) and allows one to write

$$\begin{aligned} \rho(t + \Delta t) \approx & \left[ 1 + (\mathcal{N}\Delta t + \sqrt{\mathcal{N}(q+1)}\Delta W)(\mathcal{G} - 1) \right. \\ & + \frac{1}{2} \{ (\mathcal{N}\Delta t)^2 + 2\mathcal{N}\sqrt{\mathcal{N}(q+1)}\Delta t\Delta W \\ & + \mathcal{N}(q+1)(\Delta W)^2 - \sqrt{\mathcal{N}(q+1)}\Delta W \\ & \left. - \mathcal{N}\Delta t \} (\mathcal{G} - 1)^2 + \mathcal{N}\Delta t \mathcal{D}[\hat{L}^{(p, -q/2)}] \right] \rho(t). \end{aligned} \quad (\text{A8})$$

Averaging over the uncertainty in the number of excitations added to the cavity and taking the limit  $\Delta t \rightarrow 0^+$ ,

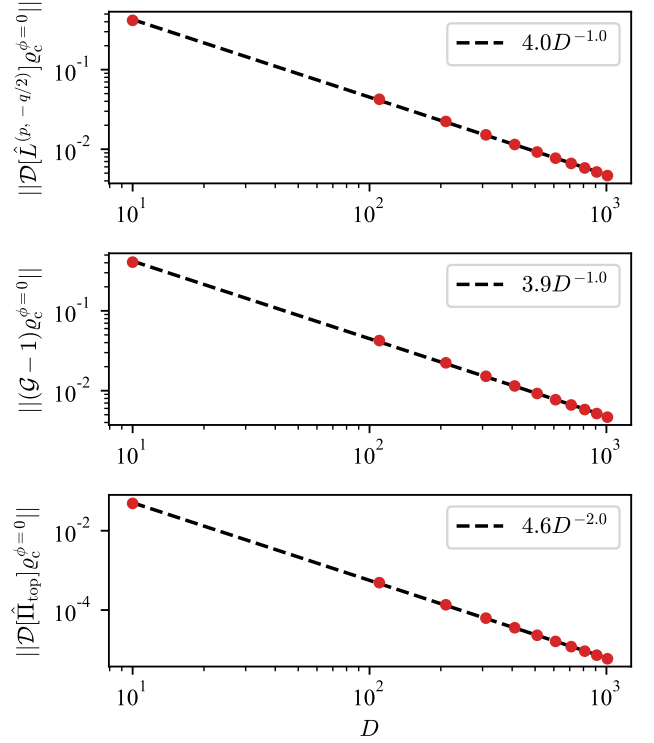


FIG. 10. Frobenius norms, defined as  $\|\hat{A}\| = (\text{Tr}\{\hat{A}^\dagger \hat{A}\})^{-1/2}$ , of the matrices  $\mathcal{D}[\hat{L}^{(p, -q/2)}]_{\varrho_c^{\phi=0}}$ ,  $(\mathcal{G} - 1)_{\varrho_c^{\phi=0}}$  and  $\mathcal{D}[\hat{\Pi}_{\text{top}}]_{\varrho_c^{\phi=0}}$  (red dots) as a function of cavity dimension,  $D$ .  $\varrho_c^{\phi=0}$  represents the pure cavity state, defined in Eq. (A6). Dashed black lines correspond to fitted power laws to this data.

one obtains the master equation

$$\frac{d\rho}{dt} = \mathcal{N} \left( (\mathcal{G} - 1) + \frac{q}{2}(\mathcal{G} - 1)^2 + \mathcal{D}[\hat{L}^{(p, q)}] \right) \rho. \quad (\text{A9})$$

To obtain Eq. (45) in the main text, we also let  $(\mathcal{G} - 1) \approx \mathcal{D}[\hat{G}^{(p, 0)}]$ . This is also justified on inspection of Fig. 10, where it is also shown that the Frobenius norm of  $\mathcal{D}[\hat{\Pi}_{\text{top}}]_{\varrho_c^{\phi=0}}$  decays much faster than that of  $(\mathcal{G} - 1)_{\varrho_c^{\phi=0}}$ .

## Appendix B: Verification of Condition 4 for the Three Families of Laser Models

In this appendix, we verify the claim in Section VI of the main text, that the families of laser models we introduced exhibit Heisenberg-limited beam coherence for certain parameter values. In that section, it was shown that the coherence of the beam scales as  $\mu^4$  for the  $p$ -,  $p, \lambda$ - and  $p, q$ -families for values  $p \gtrsim 3$ . To say that this scaling is at the ultimate limit imposed by quantum mechanics, then Condition 4 must be verified, which means that Theorem 1 applies to these families of laser models. We remind the reader that for Condition 4 to be satisfied

by a particular laser model, Eqs. (10a) and (10b) must hold.

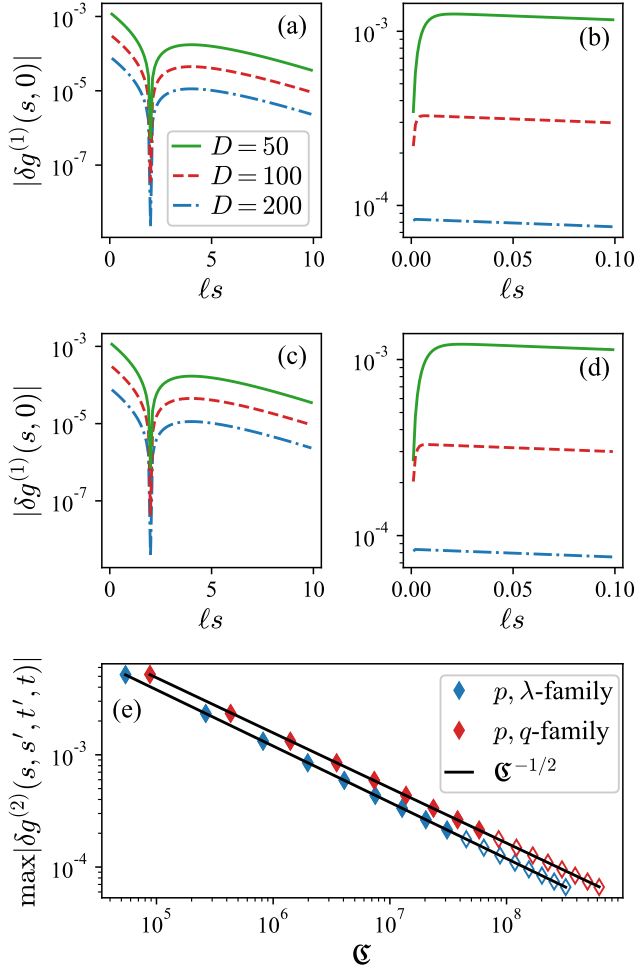


FIG. 11. (a): Deviations from the ideal laser model (a coherent undergoing pure phase diffusion) of the first-order Glauber coherence function for the family of laser models exhibiting a randomly-pumped (Markovian), non-isometric gain ( $p, \lambda$ -family) over ten coherence times. solid green, red dashed and blue dash-dotted lines correspond to cavity dimensions  $D = 50, 100, 200$ , respectively. (b): Same as that shown in (a), but over a much shorter timescale. (c,d): Same as that shown in (a,b), respectively, but for the family of laser models exhibiting a regularly-pumped (non-Markovian), quasi-isometric gain ( $p, q$ -family). (e): Global maxima of  $|\delta g^{(2)}(\tau, s', t', t)|$  versus coherence (solid diamonds) calculated for  $\{s', t', t\} \in [-\tau, \tau]$  employing interior-point optimizations of the iMPS forms for bond dimensions up to 250. Some examples of  $|\delta g^{(2)}|$  are shown for bond dimensions up to  $D = 450$  (hollow diamonds). Blue and red correspond to the  $p, \lambda$ -family and  $p, q$ -family, respectively. Black solid lines correspond to power-law fits to the data,  $|\delta g^{(2)}| = 1.2\mathfrak{C}^{-0.5}$  and  $|\delta g^{(2)}| = 1.4\mathfrak{C}^{-0.5}$ . For each of these families in plots (a-e), parameters are chosen such that beam coherence,  $\mathfrak{C}$ , is maximized for a given value of  $D$ , while  $Q$  is also minimized.

These two equations were already shown to hold for

the  $p$ -family in Ref. [1], therefore we consider only the  $p, \lambda$ - and  $p, q$ -families here, which are those that can exhibit sub-Poissonian beam photon statistics. Moreover, we constrain the parameters for each of these families to  $p = 4.1479$ ,  $\lambda = 0.5$  and  $p = 4.1479$ ,  $q = -1$ , respectively. These parameter values yield maximal beam coherence as well as a maximal degree of beam sub-Poissonianity (that is, a minimized value of  $Q$ ) for each family. Therefore, it is expected that the deviations of the first- and second-order Glauber coherence functions between these families of laser models and that of an ‘ideal’ beam would be at their greatest for these parameter values.

In order to demonstrate that Eqs. (10a) and (10b) hold for the  $p, \lambda$ - and  $p, q$ -families, we employ the same methods as those outlined in the supplementary material of Ref. [1]. With regard to Eq. (10a), which places a condition on the first-order Glauber coherence function, time-translation invariance permits a direct search for the maximum deviation over only a single time argument. In Fig. 11a and 11b, we show the quantity  $|\delta g^{(1)}(s, 0)|$ , as defined by Eq. (18), for the  $p, \lambda$ -family over two different time scales. The same is also shown in Fig. 11c and 11d for the  $p, q$ -family. As made clear from these plots, the largest deviations in the first-order coherence functions occur for each family at a short, non-zero time delay. Because this is decreasing as the cavity dimension,  $D$ , is increased, we may conclude that Eq. (10a) holds for the  $p, \lambda$ - and  $p, q$ -family for parameter values which maximize  $\mathfrak{C}$  and minimize  $Q$ .

Verifying that Eq. (10b) also holds for our two sub-Poissonian families of laser models required more sophisticated numerical techniques. This is because the problem requires an optimization over three time parameters (note that one of the four parameters in Eq. (10b) may be removed from this optimization by imposing time translation invariance). This optimization was carried out by employing a highly-scalable, non-linear optimisation routine known as the interior point method described in Refs. [56–58] to maximize Eq. (32b), along with all other non-trivial permutations of the bosonic operators [1]. As required by Condition 4, the difference between any two of the time arguments was constrained to be  $O(\sqrt{\mathfrak{C}}/\mathcal{N})$ .

From each optimization, it was found that the time arguments which maximized  $|\delta g^{(2)}(s, s', t', t)|$  were those for which there was negligible delay, for example  $(s, s', t', t) = (s, s + \epsilon, s + 2\epsilon, s + 3\epsilon)$  with  $\epsilon \rightarrow 0^+$ . In Fig. 11e we plot  $\max |\delta g^{(2)}(s, s', t', t)|$ , where  $s, s', t', t \in [-\tau, \tau]$  and  $\tau = \sqrt{3/2N\ell}$ , for the  $p, \lambda$ - and  $p, q$ -families, respectively with blue and red diamonds. In particular, the results from the optimizations are indicated by the solid diamonds, which were performed for cavity dimensions ranging between  $50 \leq D \leq 250$ . The hollow diamonds are extrapolations, where  $|\delta g^{(2)}(s, s', t', t)|$  is computed for larger cavity dimensions using the same time arguments which were obtained from the optimizations. These deviations in  $g^{(2)}$  are seen to scale as  $\mathfrak{C}^{-1/2}$ , therefore allowing us to conclude that Eq. (10b) also holds for the  $p, \lambda$ - and  $p, q$ -family of laser models and hence



Condition 4 is satisfied. This allows the statement to be made that all three families of laser models considered in

this Paper exhibit a beam coherence which is Heisenberg-limited.

- 
- [1] T. Baker, S. Saadatmand, D. Berry and H. Wiseman, “The Heisenberg Limit for Laser Coherence”, *Nat. Phys.* **17**, 179 (2020).
  - [2] L. A. Ostrowski, T. J. Baker, S. N. Saadatmand, and H. M. Wiseman, arXiv:2208.14081 [quant-ph] (2022).
  - [3] K. Chou, *et al.*, “Deterministic teleportation of a quantum gate between two logical qubits”, *Nature* **561**, 368–373 (2018).
  - [4] C. Sayrin, *et al.*, “Real-time quantum feedback prepares and stabilizes photon number states”, *Nature* **477**, 73–77 (2011).
  - [5] K. McCormic, “Quantum-enhanced sensing of a single-ion mechanical oscillator”, *Nature* **572**, 86–90 (2019).
  - [6] K. Gilmore, “Quantum-enhanced sensing of displacements and electric fields with two-dimensional trapped-ion crystals”, *Science* **373**, 673–678 (2021).
  - [7] F. Arute, *et al.*, “Quantum supremacy using a programmable superconducting processor”, *Nature* **574**, 505–510 (2019).
  - [8] H.-S. Zhong, *et al.*, “Quantum computational advantage using photons”, *Science* **370**, 1460 (2020).
  - [9] Y. Wu, *et al.*, “Strong Quantum Computational Advantage Using a Superconducting Quantum Processor”, *Phys. Rev. Lett.* **127**, 180501 (2021).
  - [10] H.-S. Zhong, *et al.*, “Phase-Programmable Gaussian Boson Sampling Using Stimulated Squeezes Light”, *Phys. Rev. Lett.* **127**, 180502 (2021).
  - [11] Q. Zhu, *et al.*, “Quantum computational advantage via 60-qubit 24-cycle random circuit sampling”, *Science Bulletin* **67**, 240–245 (2022).
  - [12] J. Preskill, “Quantum Computing in the NISQ era and beyond”, *Quantum* **2**, 79 (2018).
  - [13] D. Leibfried, R. Blatt, C. Monroe and D. Wineland, “Quantum dynamics of single trapped ions”, *Rev. Mod. Phys.* **75**, 281 (2003).
  - [14] I. Bloch, “Quantum Coherence and Entanglement with Ultracold Atoms in Optical Lattices”, *Nature* **453**, 1016 (2008).
  - [15] J. Hecht, “Short history of laser development”, *Optical Engineering* **49**, 091002 (2010).
  - [16] P. Bürgisser and F. Cucker, “Condition: The Geometry of Numerical Algorithms”, (Springer Berlin, Heidelberg, 2013).
  - [17] A. Schawlow and C. Townes, “Infrared and Optical Masers”, *Phys. Rev.* **112**, 1940 (1958).
  - [18] C. Liu, M. Mucci, X. Cao, G. Dutt, M. Hatridge and D. Pekker, “Proposal for a Continuous Wave Laser with Linewidth Well Below the Standard Quantum Limit”, *Nat. Commun.* **12**, 5620 (2021).
  - [19] A. Goldberg and A. Steinberg, “Transcoherent States: Optical States for Maximal Generation of Atomic Coherence”, *PRX Quantum* **1**, 020306 (2020).
  - [20] H. Wiseman and G. Milburn, “Noise reduction in a laser by nonlinear damping”, *Phys. Rev. A* **44**, 7815 (1991).
  - [21] T. Ralph, *Squeezing from Lasers - Quantum Squeezing*, edited by P. Drummond and Z. Ficek (Springer Berlin 2004), pp. 141–170.
  - [22] R. Glauber “The Quantum Theory of Optical Coherence”, *Phys. Rev.* **130**, 2529 (1963).
  - [23] W. Louisell, “Quantum Statistical Properties of Radiation”, (John Wiley & Sons, New York 1973).
  - [24] M. Sargent, M. Scully and W. Lamb, “Laser Physics”, (Addison-Wesley, Reading Mass., 1974).
  - [25] H. Carmichael, “Statistical Methods in Quantum Optics 1”, (Springer, 1999).
  - [26] J. Vaccaro, F. Anselmi, H. Wiseman and K. Jacobs, “Tradeoff between extractable mechanical work, accessible entanglement, and ability to act as a reference system, under arbitrary superselection rules”, *Phys. Rev. A* **77**, 032114 (2008).
  - [27] T. Baumgratz, M. Cramer and M. Plenio, “Quantifying Coherence”, *Phys. Rev. Lett.* **113**, 140401 (2014).
  - [28] A. Streltsov, G. Adesso and M. Plenio, “Colloquium: Quantum coherence as a resource”, *Rev. Mod. Phys.* **89**, 041003 (2017).
  - [29] L. Mandel, “Sub-Poissonian photon statistics in resonance fluorescence”, *Opt. Lett.* **4**, 205–207 (1979).
  - [30] L. Mandel, “Non-Classical States of the Electromagnetic Field”, *Phys. Scr. T* **12**, 34 (1986).
  - [31] X. Zou and L. Mandel, Photon-antibunching and sub-Poissonian Photon Statistics, *Phys. Rev. A* **41**, 475 (1990).
  - [32] L. Davidovich, “Sub-Poissonian processes in quantum optics”, *Rev. Mod. Phys.* **68**, 127 (1996).
  - [33] H. Wiseman, “How many principles does it take to change a light bulb ... into a laser?”, *Phys. Scr.* **91**, 033001 (2016).
  - [34] H. Wiseman and G. Milburn, *Quantum Measurement and Control*, Cambridge University Press (2009).
  - [35] A. Bandilla, H. Paul and H. Ritze, “Realistic Quantum States of Light with Minimum Phase Uncertainty”, *Quantum Optics: Journal of the European Optical Society Part B* **3**, 267 (1991).
  - [36] R. Orús, “A practical introduction to tensor networks: Matrix product states and projected entangled pair states”. *Annals of Physics* **349**, 117–158 (2014).
  - [37] I. Cirac, D. Pérez-García, N. Schuch and F. Verstraete, “Matrix product states and projected entangled pair states: Concepts, symmetries, theorems”, *Rev. Mod. Phys.* **93**, 045003 (2021).
  - [38] C. Schön, E. Solano, F. Verstraete, I. Cirac and M. Wolf, “Sequential generation of entangled multiqubit states”, *Phys. Rev. Lett.* **95**, 110503 (2005).
  - [39] C. Schön, K. Hammerer, M. Wolf, I. Cirac and E. Solano, “Sequential generation of matrix-product states in cavity qed”, *Phys. Rev. A* **75**, 032311 (2007).
  - [40] Y. Golubov, I. Sokolov, “Antibunching of photons in a coherent light source and the suppression of photorecording noise”, *Sov. Phys JETP* **60**, 234 (1984).
  - [41] Y. Yamamoto, S. Machida and O. Nilsson, “Amplitude squeezing in a pump-noise-suppressed laser oscillator”, *Phys. Rev. A* **34**, 4025 (1986).
  - [42] F. Haake, S. Tan and D. Walls, “Photon noise reduction in lasers”, *Phys. Rev. A* **40**, 7121 (1989).

- [43] M. Marte and P. Zoller, “Lasers with sub-Poissonian pump”, *Phys. Rev. A* **40**, 5774 (1989).
- [44] H. Wiseman, “Stochastic quantum dynamics of a continuously monitored laser”, *Phys. Rev. A* **47**, 5180 (1993).
- [45] M. Scully and W. Lamb, “Quantum Theory of an Optical Maser. I. General Theory” *Phys. Rev.* **159**, 208 (1967).
- [46] D. Walls and G. Milburn, “Quantum Optics”, (Springer, 2008).
- [47] T. Ralph and C. Savage, “Squeezed light from conventionally pumped multilevel lasers”, *Opt. Lett.* **16**, 1113-1115 (1991).
- [48] H. Ritsch, P. Zoller, C. Gardiner and D. Walls “Sub-Poissonian laser light by dynamic pump-noise suppression”, *Phys. Rev. A* **44**, 3361 (1991).
- [49] J. Bergou, L. Davidovich, M. Orszag, C. Benkert, M. Hillery, and M. O. Scully, “Role of pumping statistics in maser and laser dynamics: Density-matrix approach”, *Phys. Rev. A* **40**, 5073 (1989).
- [50] C. Benkert, M. O. Scully, J. Bergou, L. Davidovich, M. Hillery, and M. Orszag, “Role of pumping statistics in laser dynamics: Quantum Langevin approach” *Phys. Rev. A* **41**, 2756 (1990).
- [51] J. Bergou and M. Hillery, “From sub-Poissonian to super-Poissonian pumping in the micromaser: Corrections to reservoir theory”, *Phys. Rev. A* **49**, 1214 (1994).
- [52] L. Davidovich, S. Zhu, A. Khoury and C. Su, “Suitability of the master-equation approach for micromasers with non-Poissonian pumping”, *Phys. Rev. A* **46**, 1630 (1992).
- [53] L. Susskind and J. Glogower, “Quantum mechanical phase and time operator” *Physics Physique Fizika* **1**, 49 (1964).
- [54] H. Wiseman, “Light amplification without stimulated emission: Beyond the standard quantum limit to the laser linewidth” *Phys. Rev. A* **60**, 4083 (1999).
- [55] H. Wiseman and J. Vaccaro, “Inequivalence of Pure State Ensembles for Open Quantum Systems: The Preferred Ensembles Are Those That Are Physically Realizable”, *Phys. Rev. Lett.* **87**, 240402 (2001).
- [56] R. Byrd, M. Hribar and J. Nocedal, “An interior point algorithm for large-scale nonlinear programming”, *SIAM J. Optimiz.* **9**, 877-900 (1999).
- [57] R. Byrd, J. Gilbert and J. Nocedal, “A trust region method based on interior point techniques for nonlinear programming”, *Math. Program.* **89**, 149-185 (2000).
- [58] R. Waltz, J. Morales, J. Nocedal and D. Orban, “An interior algorithm for nonlinear optimization that combines line search and trust region steps”, *Math. Program.* **107**, 391-408 (2006).